All-sky imaging techniques to study the upper atmosphere

Carlos Martinis
Center for Space Physics
Boston University

Imaging science

OUTLINE

1. Introduction
2. Airglow emissions
3. All-sky imaging issues **(with Jeff Baumgardner)**
4. All-sky imaging of mesospheric and thermospheric processes
5. Narrow field of view imaging and Beyond the Earth's atmosphere
6. Summary

Introduction

* The study of atmospheric emissions was initiated in the 30's by Rayleigh, Cabannes, Barbier. Further progress was established by Roach and Meinel in the '50s.

* In the early '70s Eather and Mende combined existing photoelectric photometers with all-sky optics to look at the aurora.

* For equatorial and low latitude studies of faint airglow emissions the first observations were made by Weber in 1978. 2.5 sec exposures; the resulting TV frames were recorded on videotape and by photographing the TV monitor

(Weber et al., 1978)

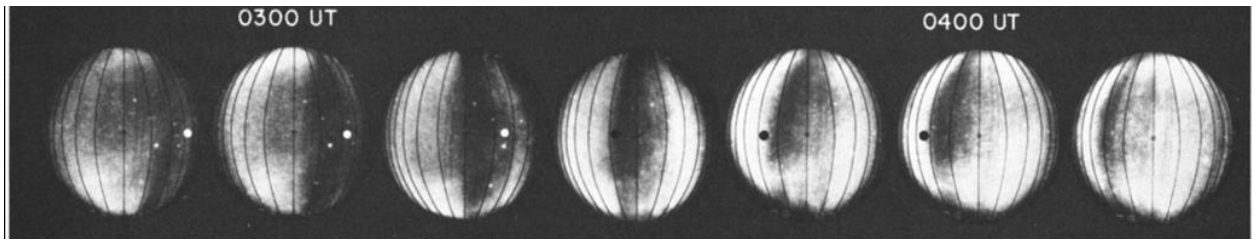

(Mendillo and Baumgardner, 1982)

* In 1981, Mendillo and Baumgardner installed an all-sky imager at Ascension Island. The output phosphor was then imaged on to 35-mm film

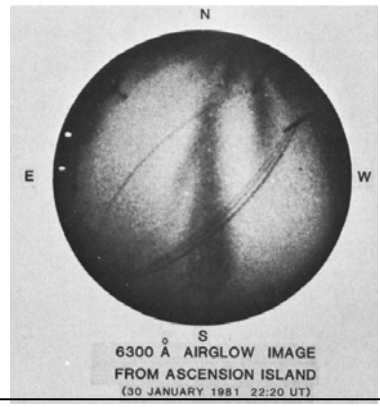

*** Since these original studies in the late 70s and early 80s all-sky imaging techniques proved to be extremely valuable when studying the evolution of processes in the mesosphere, thermosphere, and ionosphere. *2D imaging literally adds a second observational dimension to line-of-sight (e.g., radar, lidar) or in situ (e.g., rocket and satellite) measurements.***

Typical configuration of an imaging system

Front lens
(narrow, all-sky)

Optical system
(lenses, filters)

Detector
(TV, film, CCD)

1970s TV

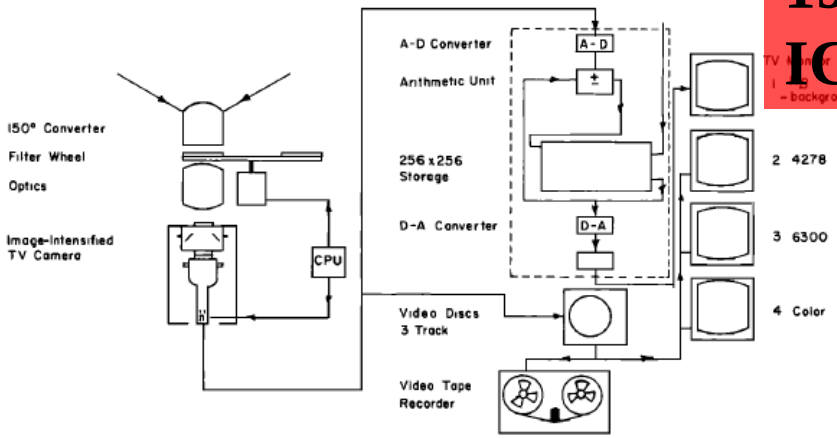

Fig. 1. Schematic representation of the all-sky monochromatic imaging system Wide field of view optics form an i of the sky through four interchangeable narrow band filters on the photocathode of the image intensifier tube. The i intensifier is coupled to the TV camera, which takes time exposures of the intensified image. A single TV scan is recorde each exposure on storage video discs and on video tape. The Hβ picture is processed by digital processor and is corr for background contamination. A minicomputer (CPU) controls the sequencing of the system. Black and white and monitor displays permit real time monitoring of auroras in each wavelength band.

1980s-1990s ICCDs

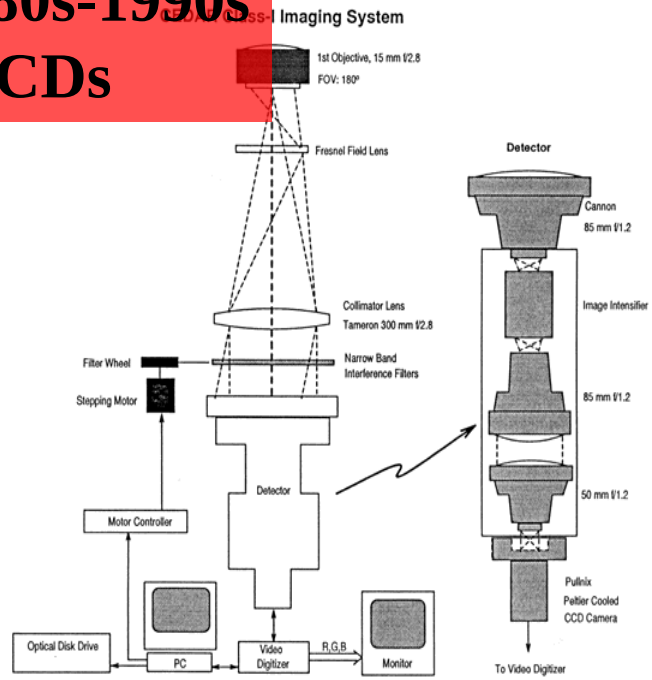

1990s-CCDs

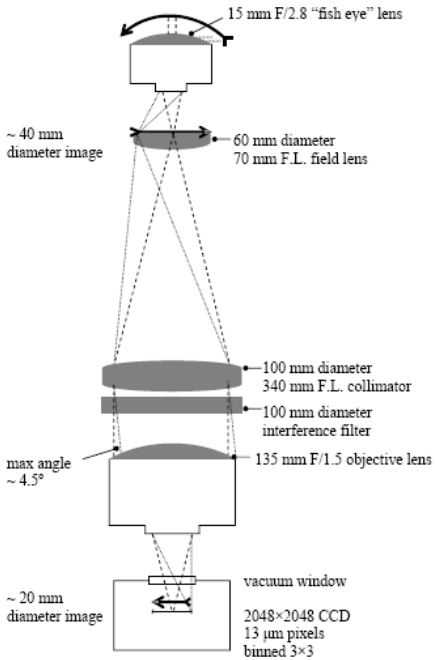

CCDs (charged coupled devices)

A CCD is basically a 2D array of photosites on a silicon substrate. **Light falling on the CCD is recorded as an electrical signal by converting photons to electrons.**

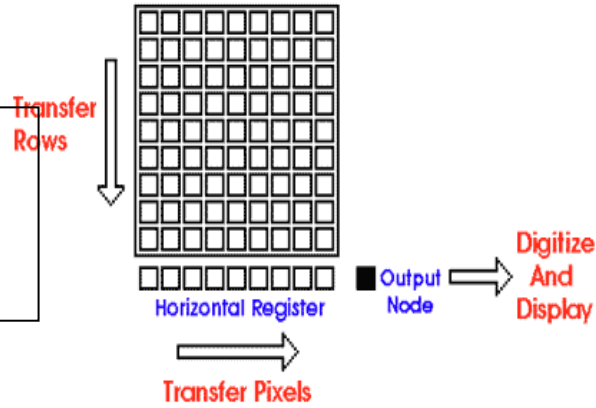

* Intensified CCD (ICCD):

First applications for aeronomy observations at low latitudes

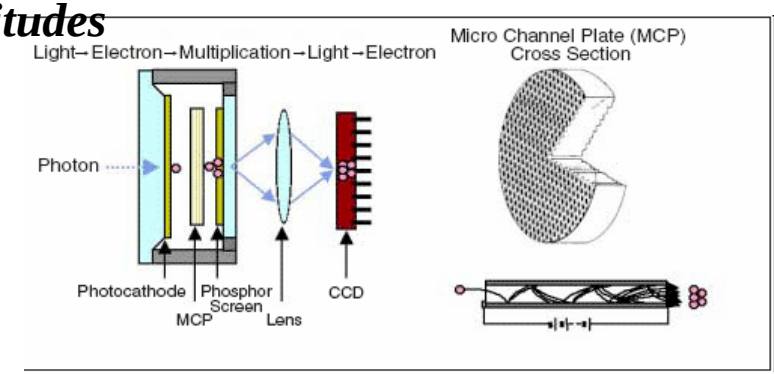

Fig. 6 Basic princi

* Bare CCDs: higher QE;

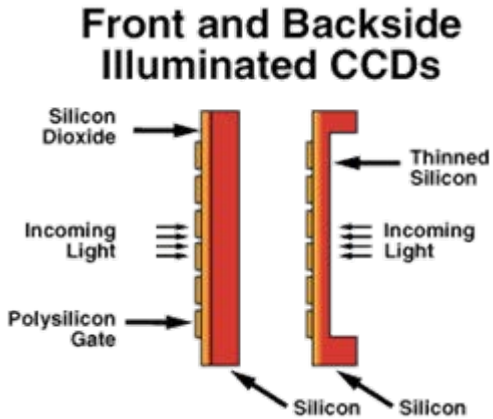

http://photomet.com

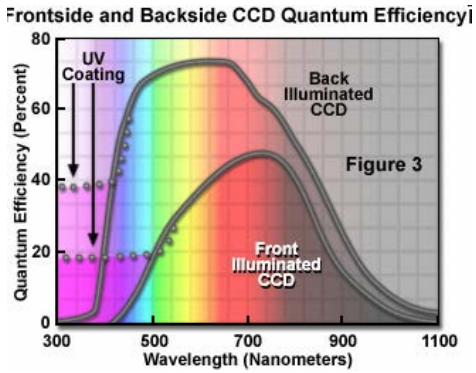

http://micro.magnet.fsu.edu

* EMCCDs (electron multiplying CCDs):

Most EMCCDs utilize a Frame Transfer CCD structure that features two areas – the sensor area and the storage area.

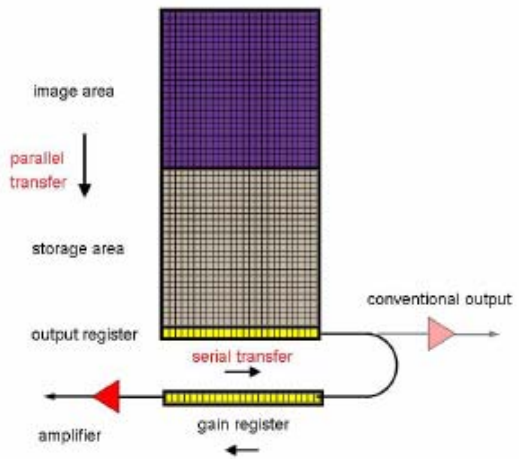

from McWhirter,'08

NOISE

Image signal: from the source and background (S+B)
and Thermal signal: thermal activity of the semiconductor (D)

Noise: In addition to the signal we are interesting there is noise. Noise is uncertainty in the true value of the pixel , which shows itself as variability in the results of a given measurement. The Signal to Noise Ratio (SNR) is defined as the ratio between a given signal and the noise associated with that signal.

* **Photon noise:** The incoming photons ***S*** have an inherent noise; follow Poisson statistics, random process.

***Thermal noise**: Noise resulting from thermally generated electrons; dark signal. The dark signal adds to your measured signal (S+B).

* **Readout noise:** inherent property of the CCD sensor. Readout is the process by which data are taken from the pixels of the CCD and stored in computer memory.

***Quantization noise:** is generated by the signal coming from the CCD digitization

$$SNR = \frac{S}{\sqrt{(S+B)+D+R}}$$

S ≡ signal

B ≡ background

D ≡ dark or thermal noise

R ≡ read out noise

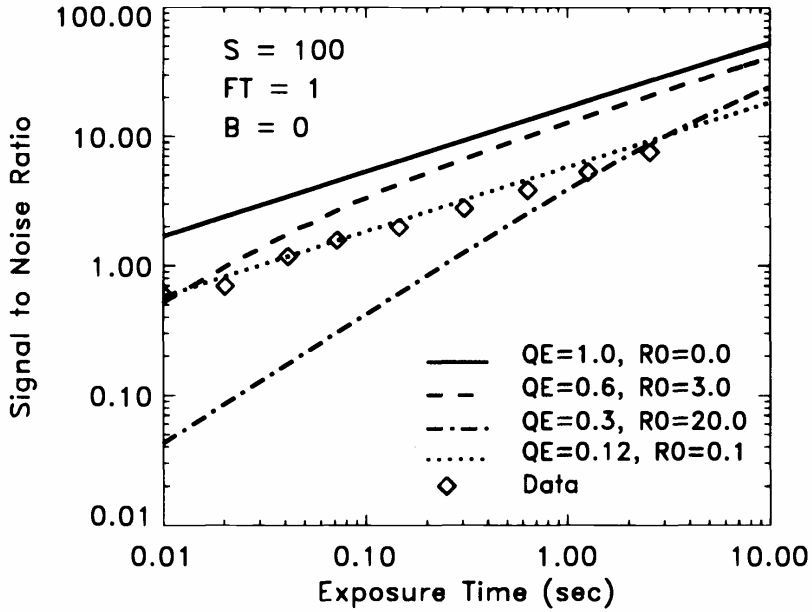

(a)

Large signal on small background (ex. Airglow/aurora during night time) S = 300R; B =3R/Å

$$SNR = \frac{S}{\sqrt{(S+B)+D+R}}$$

Large signal on large background (Daytime/ twilight Airglow/ auroral emissions) S= 3 kR; B =1-5 MR/Å

$$SNR = \frac{S}{\sqrt{(S+B)+D+R}}$$

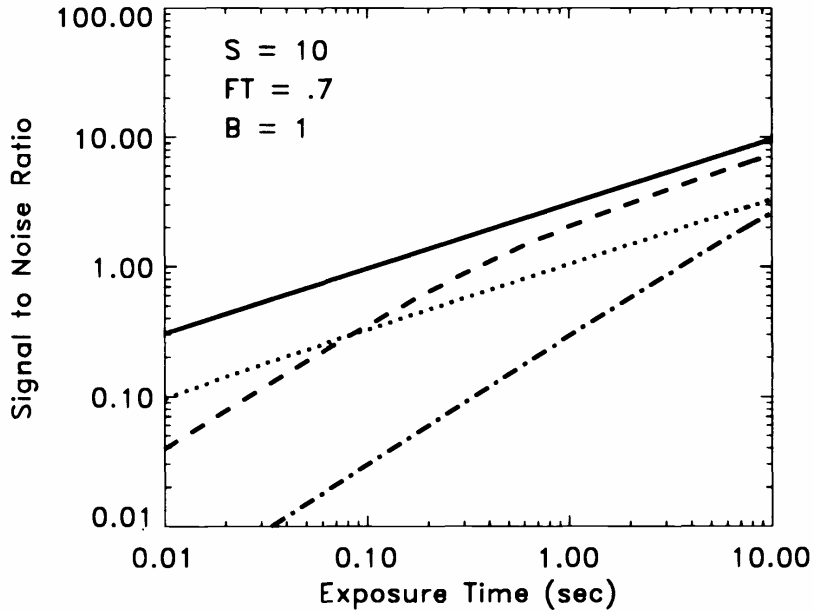

From Duggirala's CEDAR tutorial, 2003

From Baumgardner et al., 1993

In EMCCDs:

Spurious noise (Clock Induced Charge) and Noise Factor (Amplification noise)

$$F^2 = \frac{\delta_{out}^2}{M^2 \delta_{inp}^2} \qquad \frac{S}{N} = \frac{S}{\sqrt{F^2(S + B + D + CIC) + R/M^2}}$$

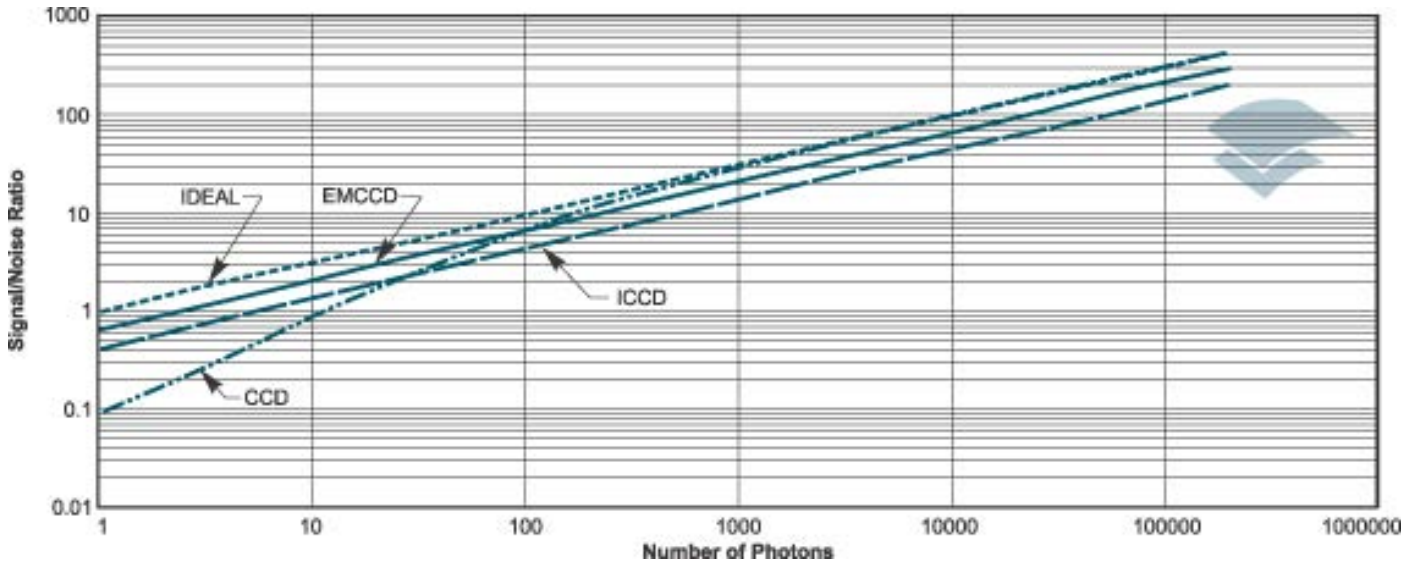

http://www.Andor.com

	Ideal	**CCD**	**EMCCD**	**ICCD**
Quantum Efficiency (D_{QE})	100%	93%	93%	50%
Readout Noise	0	10	60	20
Gain	1	1	1,000	1,000
Spurious Noise	0	0.05	0.05	0
Dark Noise	0	0.001	0.001	0.001
Noise Factor	1	1	1.41	1.6

Airglow

Airglow is a term that refers to an optical emission from excited atmospheric species

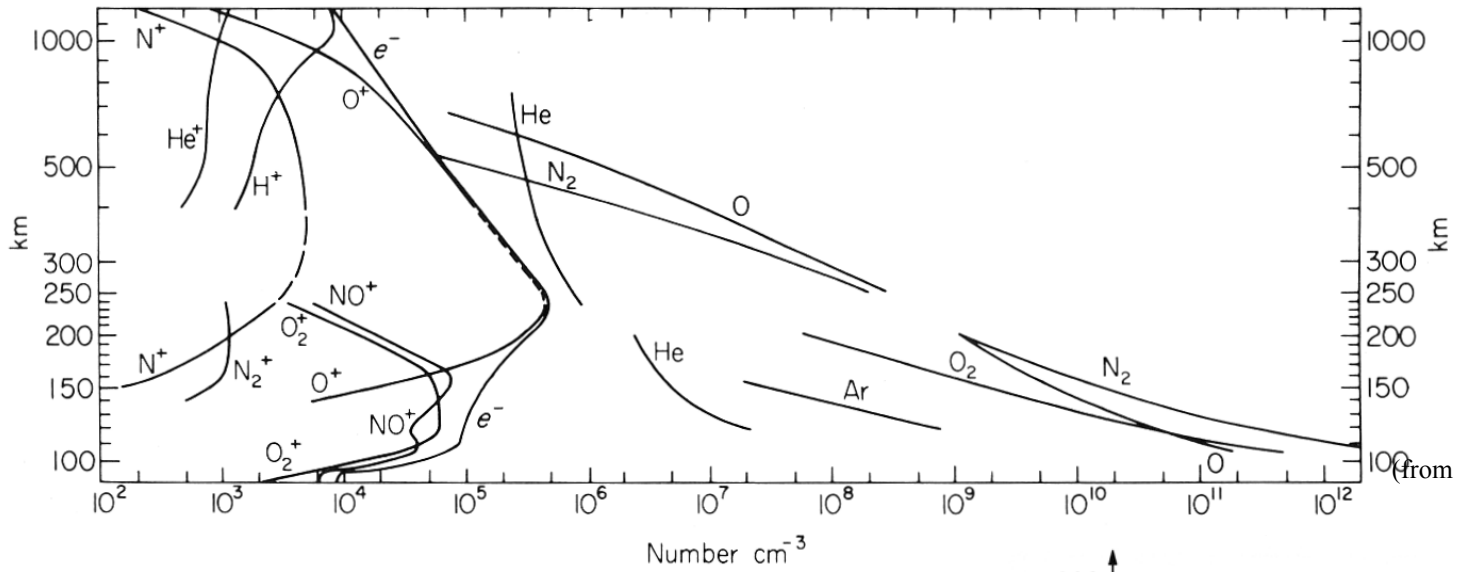

(from Johnson, 1969)

Solar EUV radiation ionizes neutral species in the upper atmosphere

Main neutrals: N_2 , O_2 , O

Main ions: NO^+ , O_2^+ , O^+

E region: photochemistry is dominant

F region: transport is important

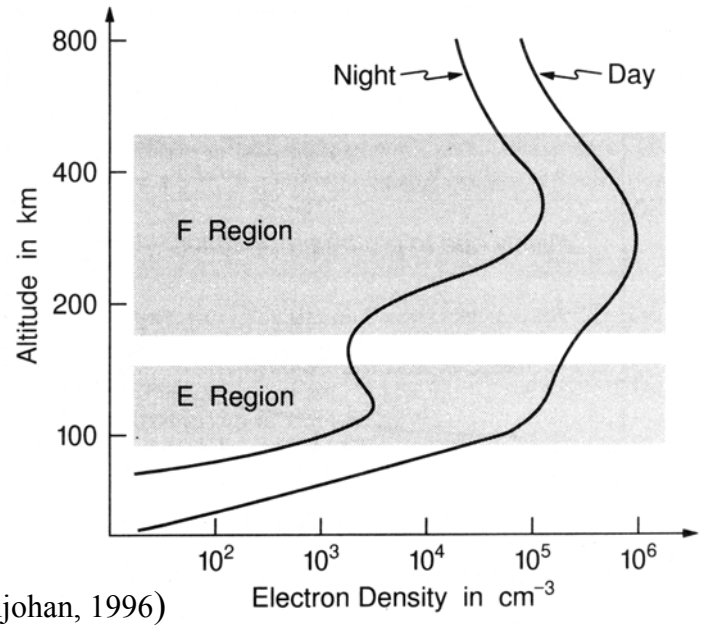

(from Baumjohan, 1996)

Nightglow spectrum

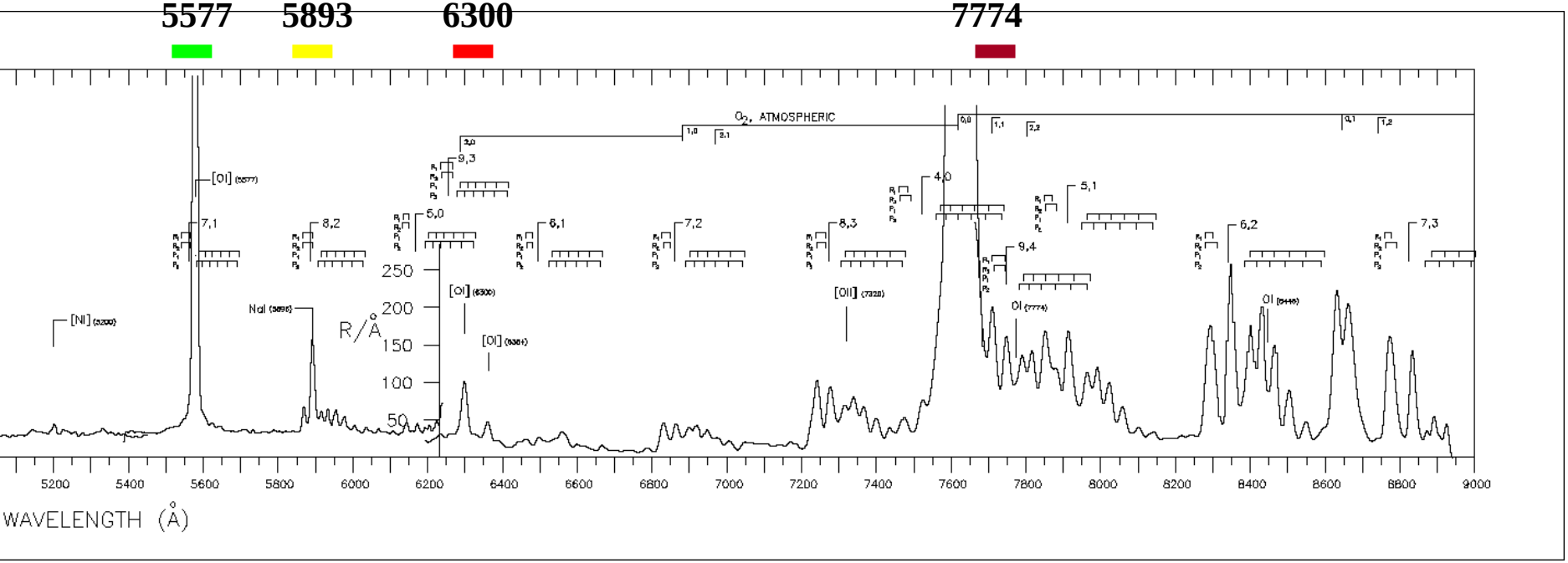

http://glo.lpl.arizona.edu/glo/

The GLO (Arizona Airglow Experiment) instrument has a set of imaging spectrographs that simultaneously observe the entire wavelength range from 1150Å to 9000Å at a resolution of ~5Å in the UV and visible to ~10Å in the near IR.

* All-sky imager measurements in the mesosphere : GWs, Bores

Typical Airglow emissions in the mesosphere:

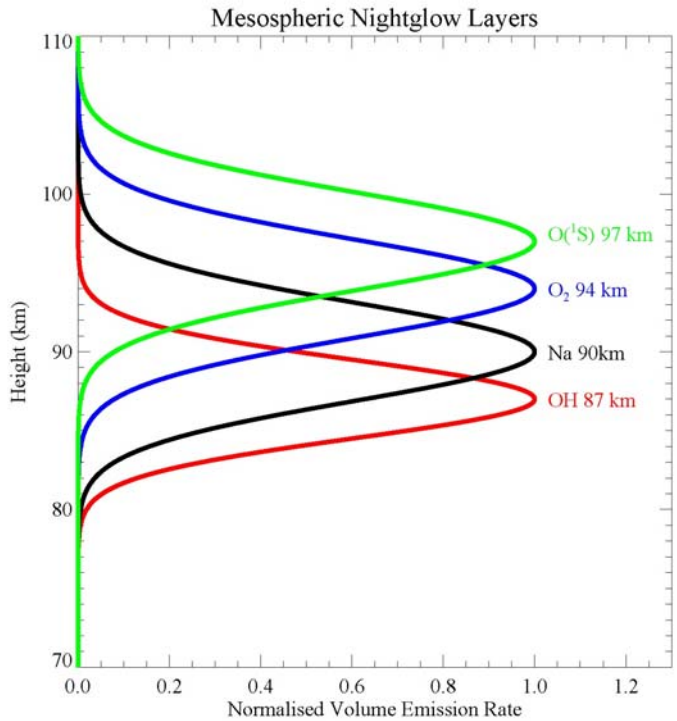

1. Hydroxyl (OH). Numerous Meinel bands range from visible to the infrared.

2. Neutral Sodium (Na). Line doublet 589.0 & 589.6 nm.

3. Molecular Oxygen (O2). O2(0-1) band is centered at 866.0 nm.

4. Neutral atomic oxygen (O(^{1}S)). Line at 557.7 nm.

Most comes from the mesosphere near 96 km via the three-body Barth reaction

* Processes measured with all-sky imagers in the low and mid latitude F region: ESF; MSTIDs; BW

The typical airglow signatures in the thermosphere correspond to neutral O emissions at 6300 Å and 7774Å

* **7774Å** emission is caused by the radiative recombination of O^+

$$O^+ + e^- \rightarrow O^* + h\nu_{7774}$$

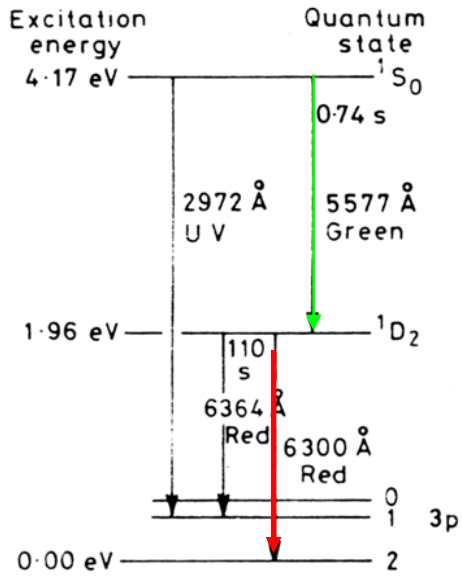

* The so-called oxygen red line at 6300 Å (OI 6300 Å) represents the spontaneous de-excitation of atomic oxygen from the ^{1}D state to the ^{3}P ground state.

O(^{1}D) is produced mainly by two processes involving O^+. The first one with O_2 and the second one, less important, with N_2

$$O_2 + O^+ \xrightarrow{\gamma_1} O_2^+ + O \qquad O_2^+ + e^- \xrightarrow{\alpha_1} (2-\beta_1)O + \beta_1 O(^1D)$$

* O(^{1}D) states de-excite by *quenching* with neutrals through

$$O(^1D) + O_2 \xrightarrow{\kappa_2} O_2 + O(^3P)$$

$$\boxed{L_q = d_D[O(^1D)]}$$

with $d_D = \kappa_1 [N_2] + \kappa_2 [O_2] + \kappa_3 [e^-] + \kappa_4 [O]$

* O(^{1}D) states can de-excite also by *spontaneous emission* of a photon

$$\boxed{L_s = A_D[O(^1D)]}$$

$A_D = A_{6300} + A_{6364}$

$$[O(^1D)] = \frac{\overbrace{\left(\beta_1\alpha_1[O_2^+] + \beta_2\alpha_2[NO^+]\right)[e^-]}^{production}}{\underbrace{A_D + d_D}_{loss}}$$

$$\boxed{O(^1D) \xrightarrow{A_{6300}} O(^3P) + (h\nu)_{6300}}$$

$$\varepsilon_{6300} = \frac{d[h\nu]_{6300}}{dt} = A_{6300}\left[O(^1D)\right]$$

$$\varepsilon_{6300} = A_{6300}\frac{(\beta_1\alpha_1\gamma_1[O_2] + \beta_2\alpha_2\gamma_2[N_2])[e^-]}{A_D + d_D}$$

*** The emission is limited to a relatively narrow layer between 250 and 300 km. For comparison, ε_{7774} is proportional to $[O^+]$ $[e^-]$.**

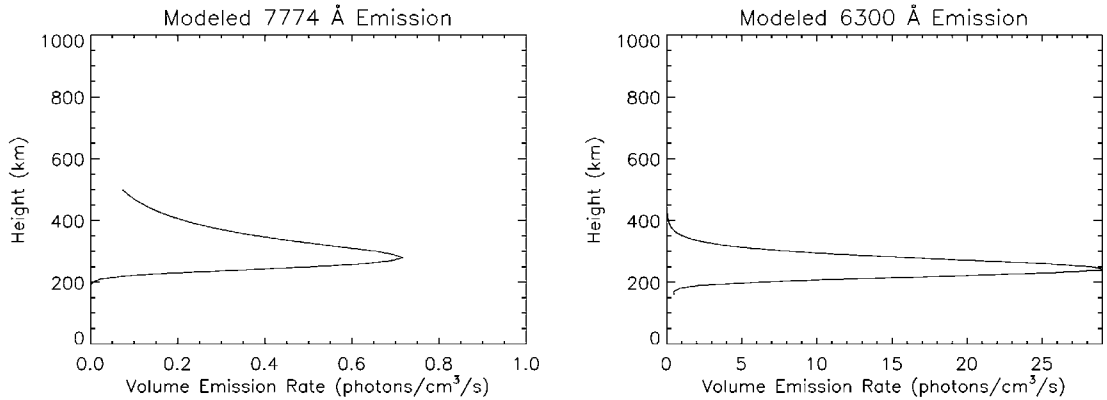

The integral with height of ε_{6300} gives the total vertical column emission rate in phot/cm$^2 \cdot$ sec. The Rayleigh is defined as 10^6 phot/cm$^2 \cdot$ sec, so the quantity we measure, expressed in Rayleighs is:

$$I_{6300}(Rayleighs) = 10^{-6}\int \varepsilon_{6300}\,dh$$

*** Combining brightness of these two emissions:**

$$h_{\max} \propto \frac{\sqrt{I_{7774}}}{I_{6300}}$$

Tinsley, 1973; Makela et al, 2001

How to set up an all-sky imager?

The system you build/buy will depend on your specific needs:

* **Narrow field of view (8^o, 19^o, 47^o) :** Sprites; Aurorae; equatorial ionospheric irregularities; planetary imaging.

* **Wide angle FOV (180^o) ,** a.k.a ***all-sky imaging:*** Equatorial (ESF), and midlatitude (MSTIDs) ionospheric irregularities; aurorae; mesospheric neutral processes (gravity waves, bores), etc.

* **Fast read out noise:** for dynamic processes, ICCDs; EMCCDs

What can you do?

1. Standard systems: Keoscientific.
2. Do it yourself:

* Cameras: Andor, Apogee, Finger Lake, Hamamutso, Princeton, etc.
* Lenses: surplus/used market.
* Filters: Andover, Barr, Knightoptical, Melles Griot, etc.

* The idea is to use large F/# (3.5 to 5.6) optics to bring the image to your optical system, and then use a small F/# (0.95 to 1.5) re-imaging lens to bring it to the CCD detector.

*** Fish-eye lens**: limited options: Mamiya 24 mm/F4; sigma 15 mm/F2.8; Mamiya 24mm/F5.6. Typical image sizes from a fish-eye lens are **40, 70, and 92 mm.**

*** Filter size**: typical 3'' diameter, but better 4'' diameter (more expensive) → smaller angles.

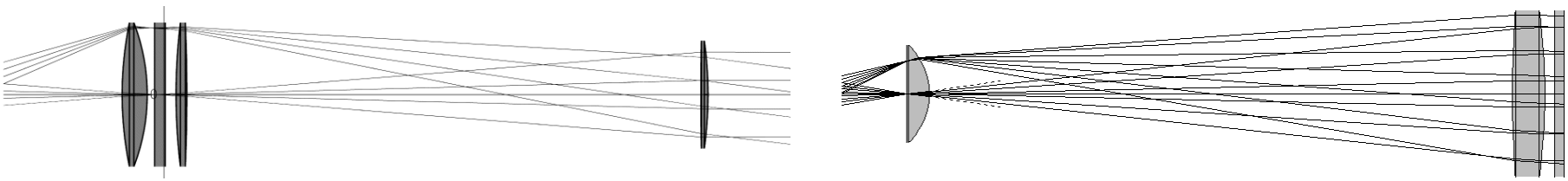

* Telecentric or Collimating configuration

Courtesy of J.Baumgardner

➢ ***Given a CCD , what is the 'plate scale' of the system***?,

- 180º are covered by 2048 pixels, then the area covered is **~0.088º/pix**
- If binned 3x3, 180º are covered by 682 pixels then: **~ 0.26º/pix**

Sensitivity increases by a factor of 9 , but resolution decreases by 3

* Narrowband Filters (FWHM ~ 10-15 Å)

Also called bandpass or interference filters, they are optical filters that reflect one or more spectral bands/lines and transmits others.

$$\lambda_\theta = \lambda_o \left[1 - \frac{n_o}{n_*} \sin^2 \theta \right]^{1/2}$$

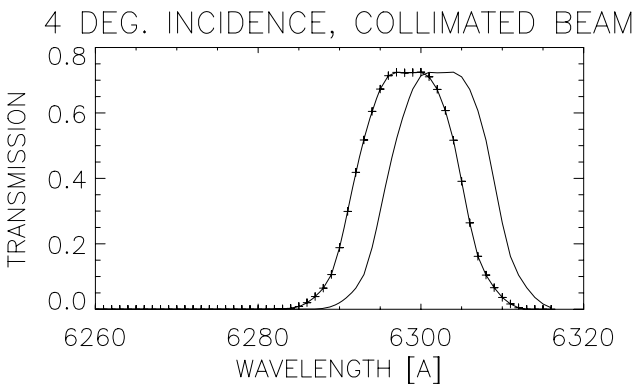

Courtesy of J. Baumgardner

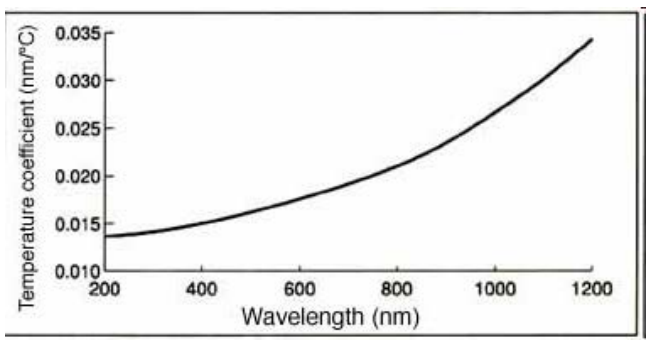

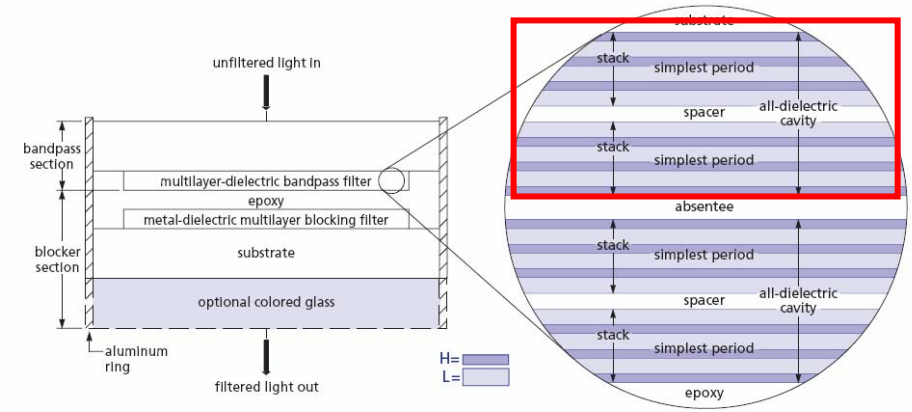

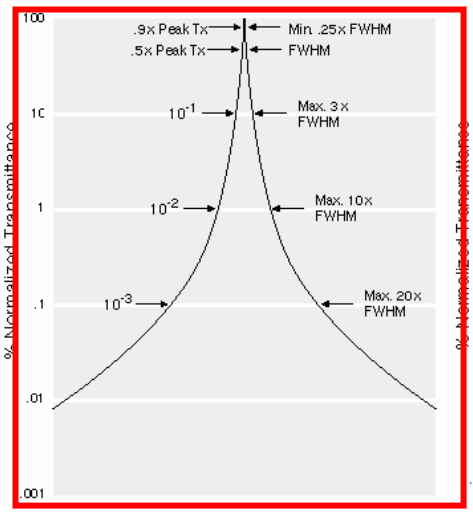

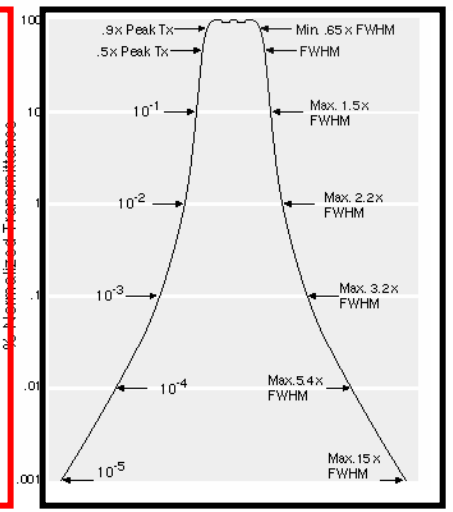

From http:/ MellesGriot.com

For a 10º change in T
630.0 nm ~ .15 nm

*** Van Rhijn effect**

slant path effect that enhance brightness due to increase in optical path length through the emission layer .

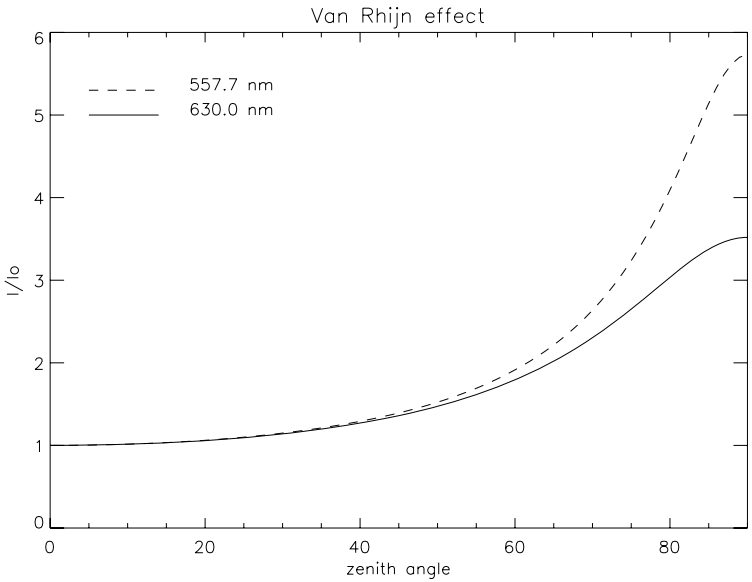

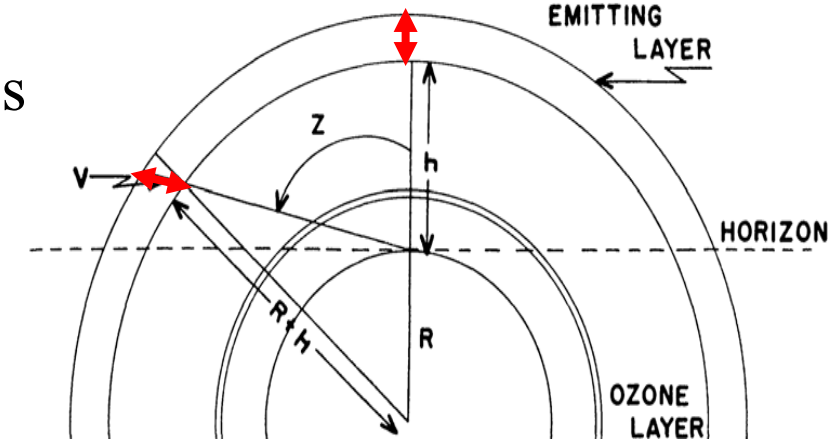

$$V = \frac{1}{\sqrt{\{1 - [R/(R+h)]^2 \sin^2 z\}}}$$

From Roach and Meinel, ApJ, 1955

*** Vignetting**

the off-axis response of the imaging system that reduces brightness at the rim of the fisheye lens toward the edge of the FOV

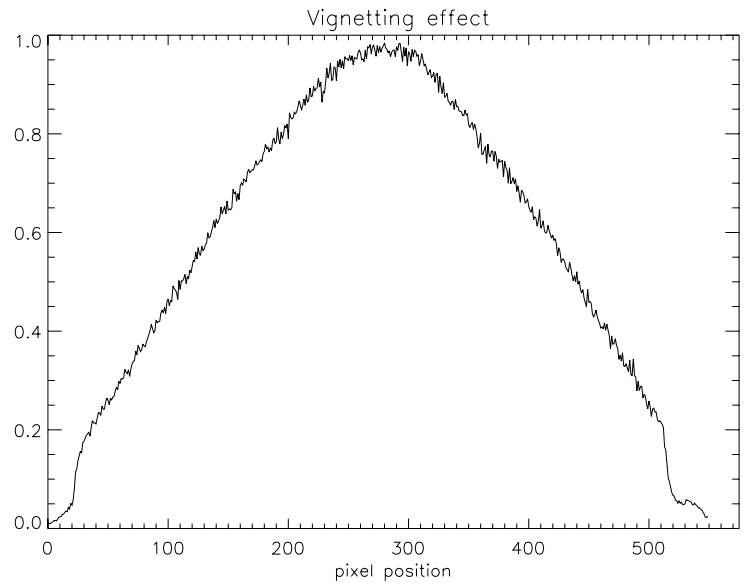

The two effects act in opposition, but vignetting tends to exceed van Rhijn enhancement at the edges

*** Calibration:**

* It is typical to use a tungsten lamp whose brightness in R/Å (or (R/nm) has been cross-calibrated with a radioactive C^{14} light source.

This source can be directly compared to the C^{14} source only over ~100 nm near 620 nm.

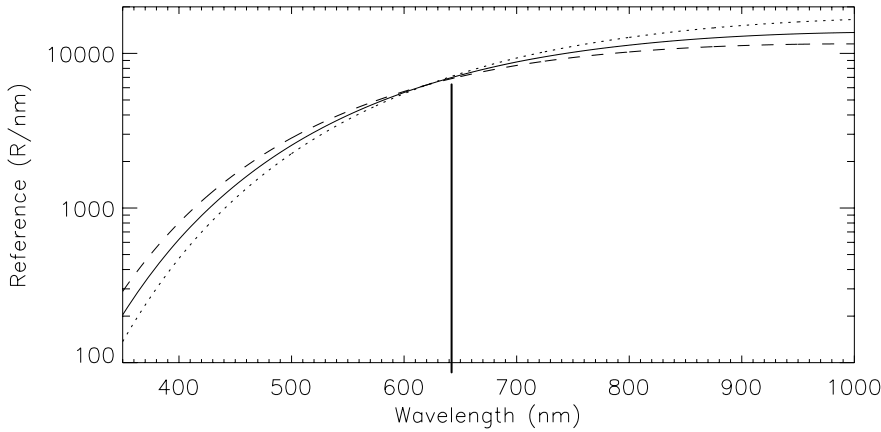

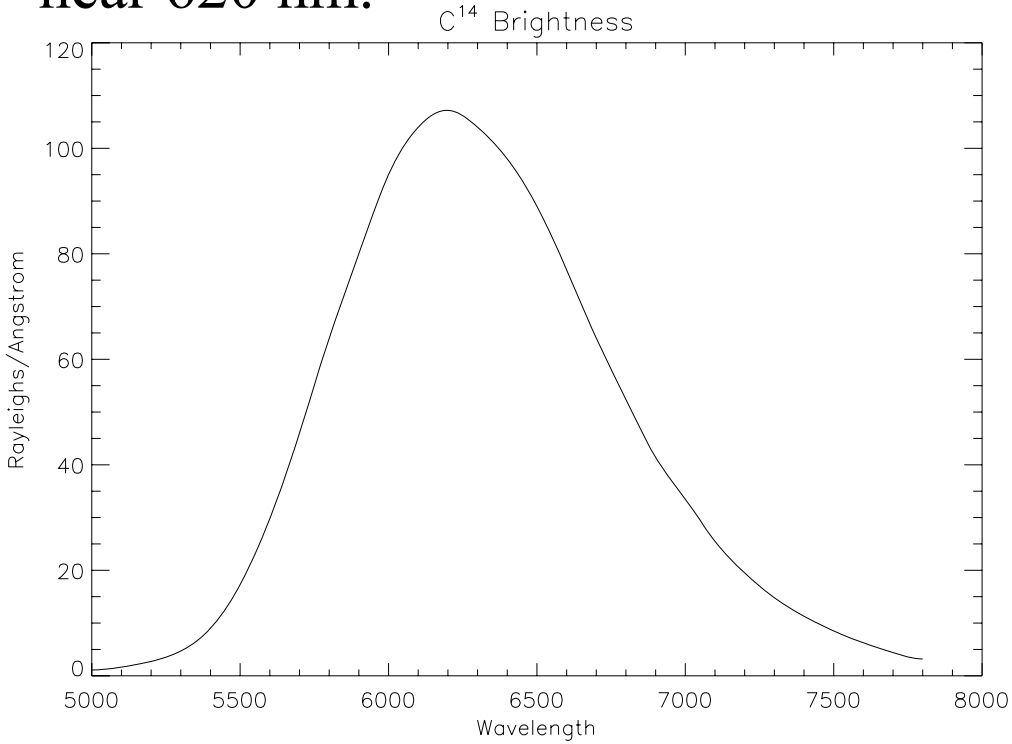

Sensitivity

*fact_C^{14}_{6300} =(C^{14}(6300) /Im_brightness1)*area

* fact_$lamp_{6300}$ =(lamp(6300) /Im_brightness2)*area

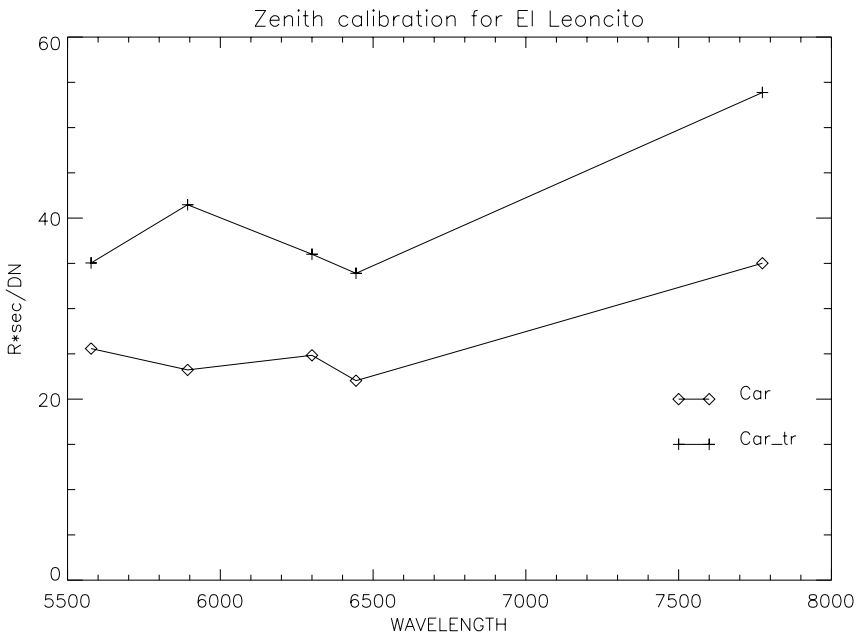

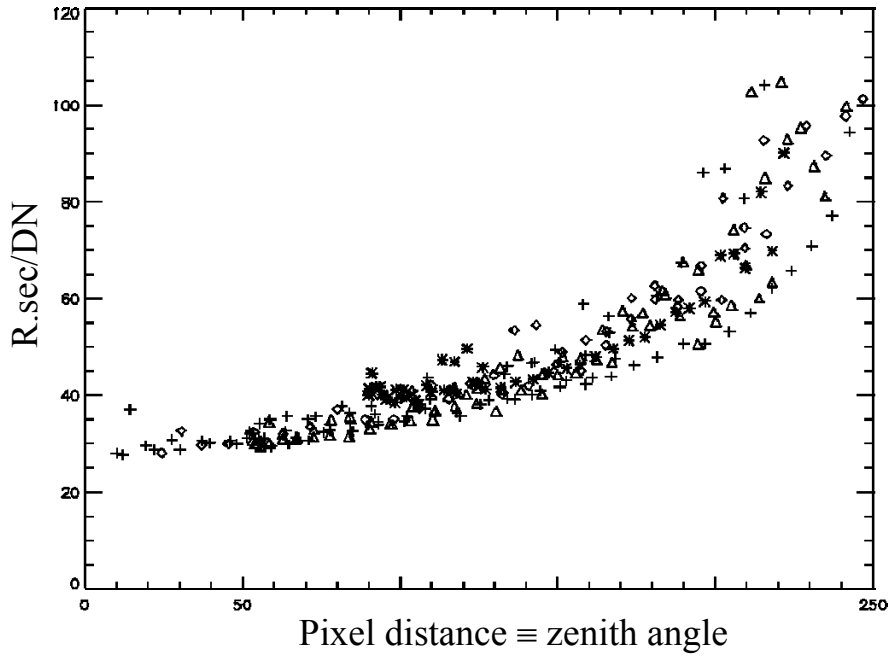

Using a C^{14} source, we obtain a zenith calibration factor that is used to calibrate the image at different zenith angles considering vignetting and assuming an extinction model

Another method implies using standard stars. The resulting curve **includes** vignetting and extinction.

Both methods show agreement at zenith:
~ 25 R.sec/DN (or 0.04 DN/R.sec)

Subtracting stars and the Milky Way from All-Sky Images

*** Stars can be filtered out using a median filter.**
* BUT large saturated areas, e.g., the Milky Way, can not be easily removed.
* Simultaneous off-band images are usually not available.
* An appropriate background image can be constructed by re-mapping the off- band image to the desired time

6300 image

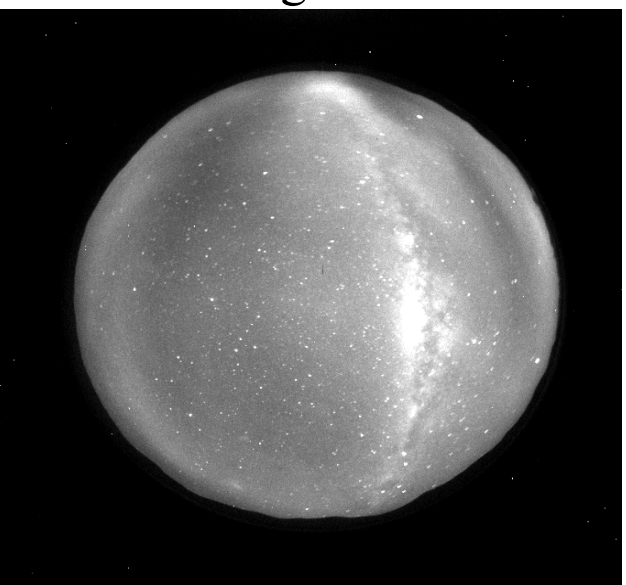

Background image

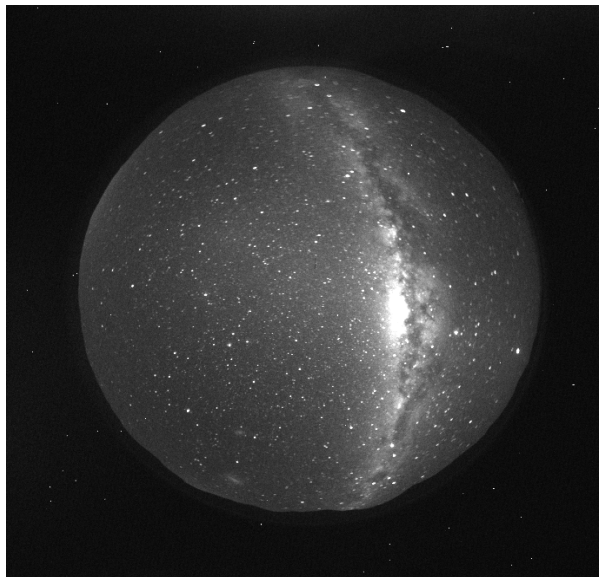

Difference

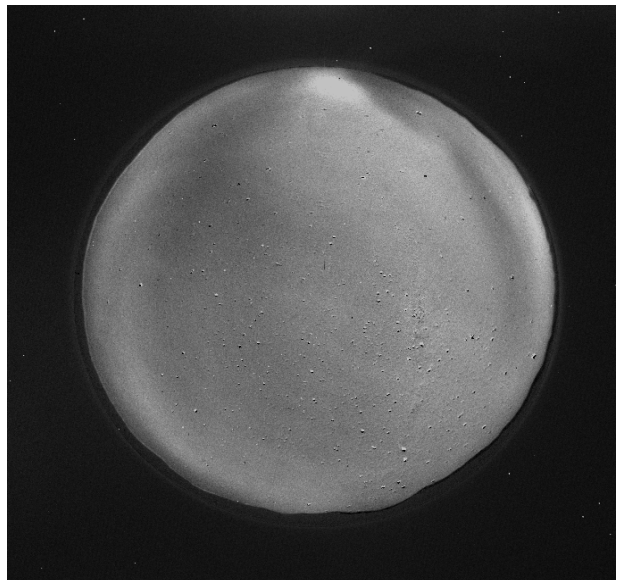

Unwarping all-sky images

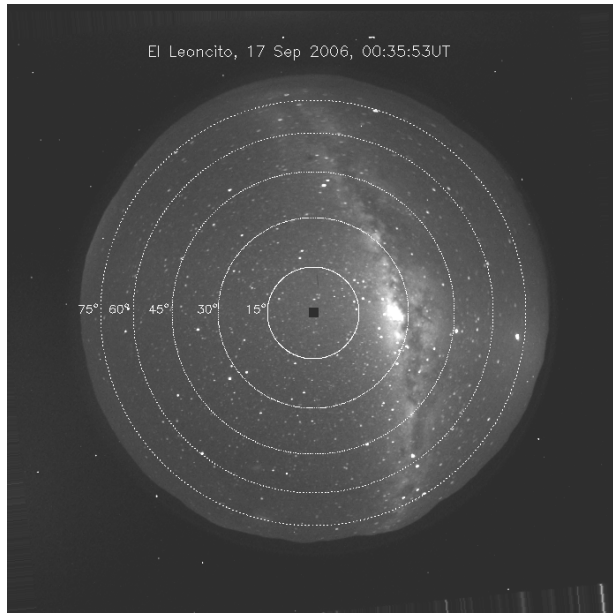

* The lens projects an image onto the CCD such that each pixel subtends an equal angle of the sky
* A zenith angle of 75^{o} encompasses approximately ± 10^{o} of latitude/longitude
* The raw image needs to be converted into geographic coordinate system, assuming an emission height. This is done by first calculating a 'distortion function' that relates zd in pixels with zd in degrees;

Raw_ Im (x, y) = Unwarped_Im (xx, yy)

Raw_ Im

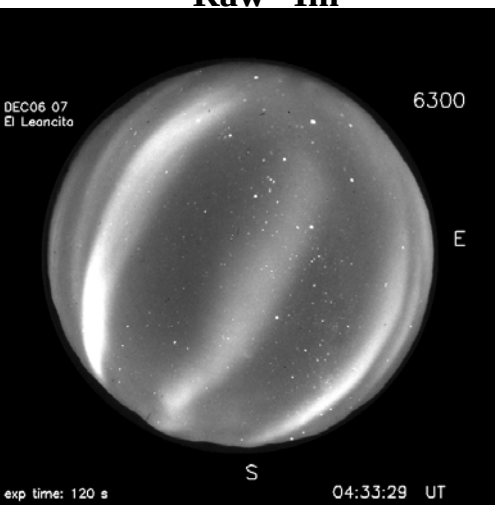

Unwarped_Im

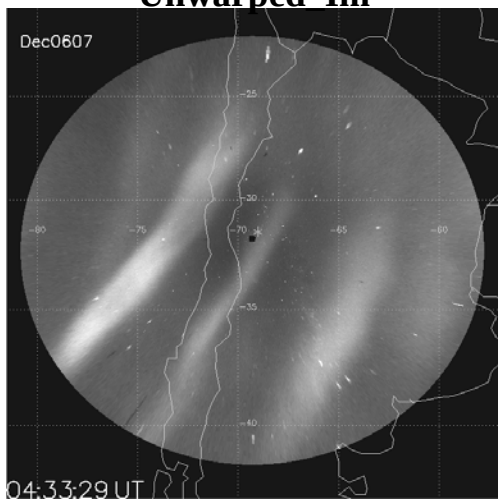

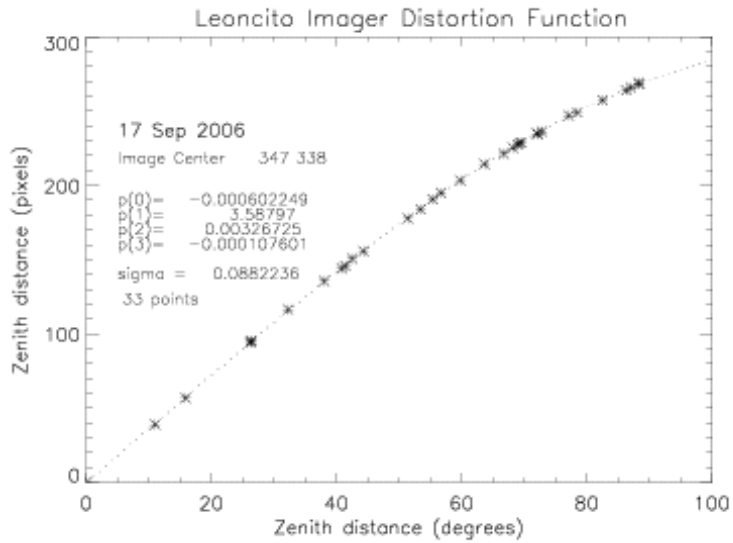

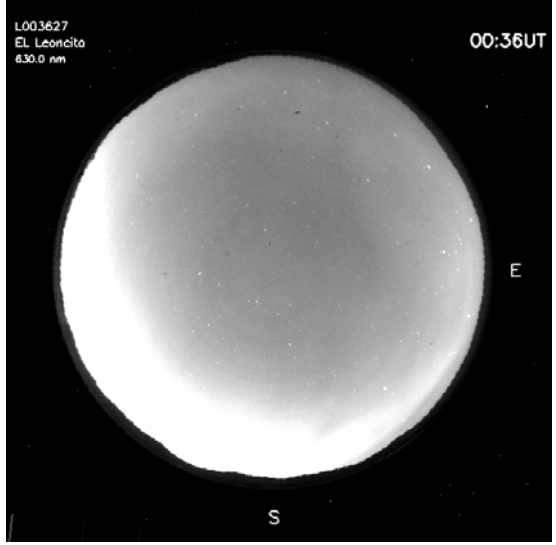

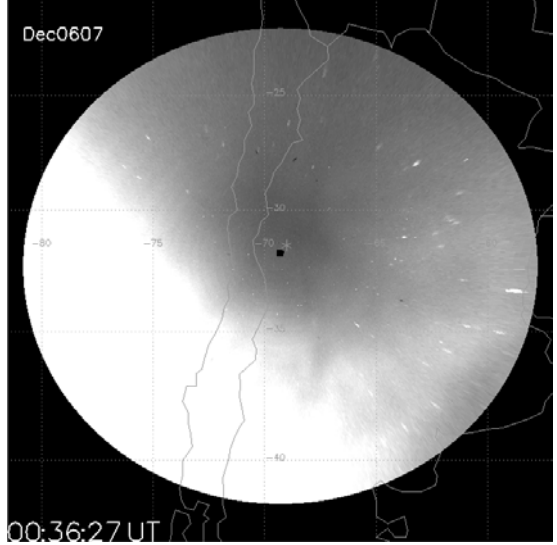

This unwarping is necessary if we are trying to find wave parameters or if we are trying to correlate in-situ or line of sight measurements

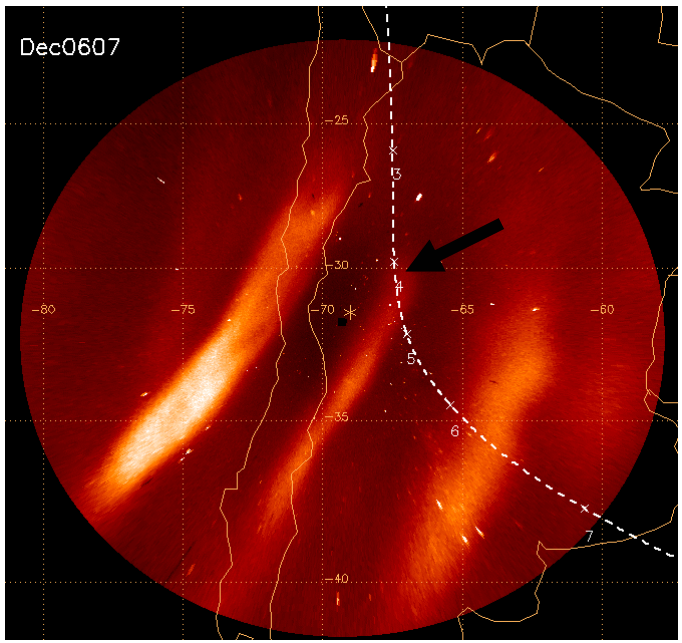

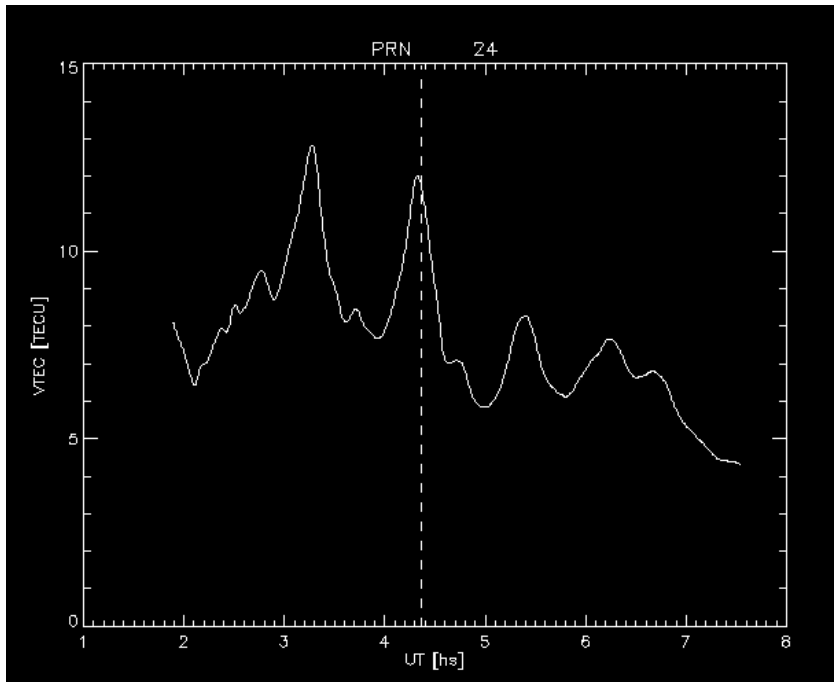

Optical Imaging of mesospheric and thermospheric processes

1. Mesospheric gravity waves and bores

2. Low and mid latitude ionospheric irregularities

3. Narrow band observations and planetary imaging

Mesospheric Gravity Waves

GWs are omnipresent in all-sky images of the night-time mesosphere

* Typical horizontal phase speeds: 20-70 ms^{-1}
* Typical horizontal wavelength: 10-50 km or more.

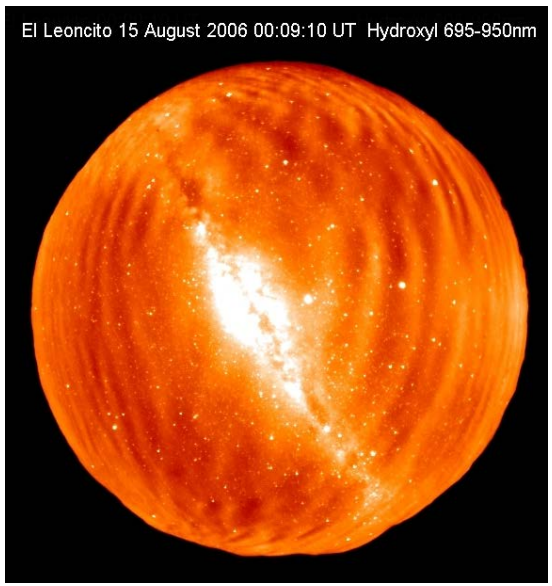

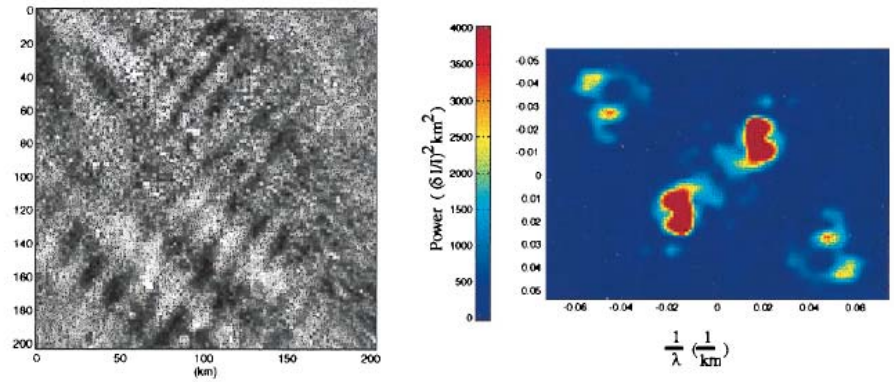

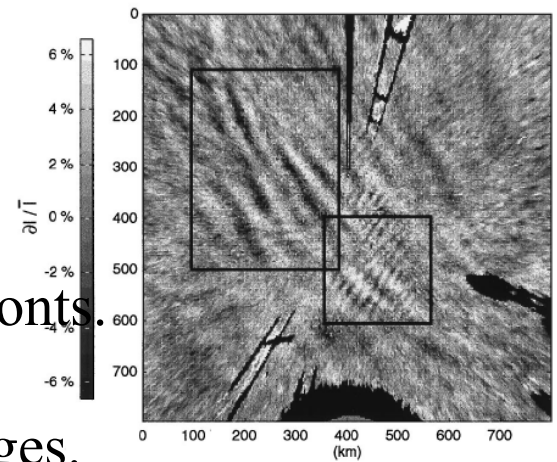

Origin:

1. Convective centers, e.g. thunderstorms, weather fronts.
2. Jet-streams.
3. Orography, e.g. winds blowing over mountain ranges.

from Garcia et al., 1997

Multi-spectral all-sky images can yield valuable information about the vertical structure of the mesopause region.

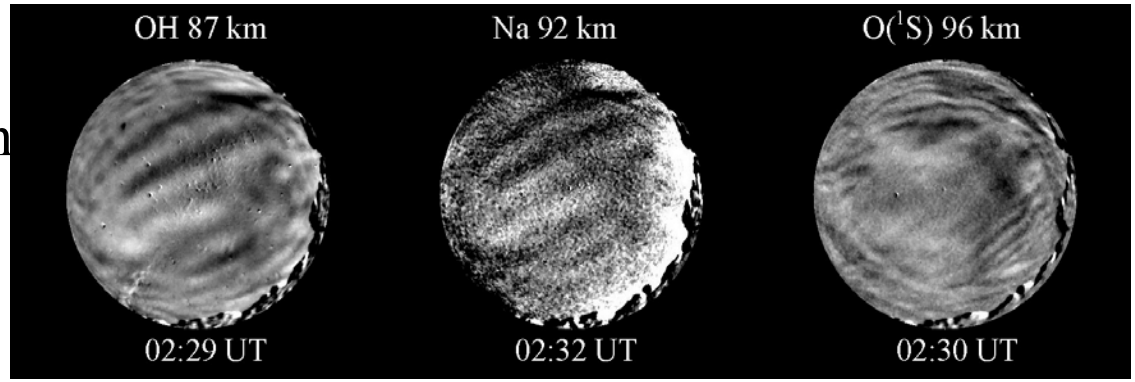

Large GWs present in the hydroxyl and Na layers at 87 km and 92 km altitude, respectively. But absent 4 km higher in the OI layer

Mesospheric Bores

* The mesospheric bore is a non-linear type of mesospheric gravity wave.

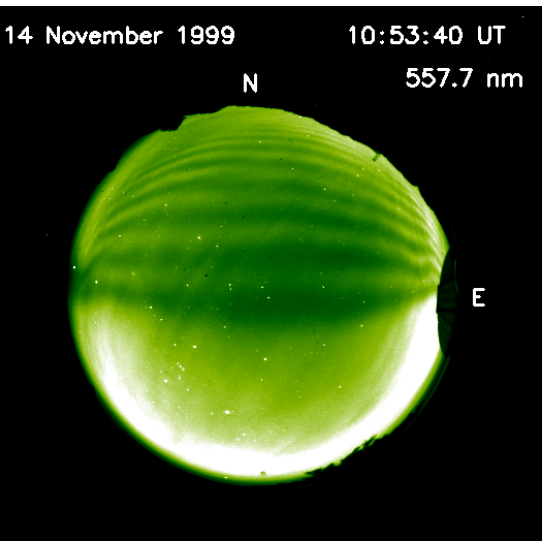

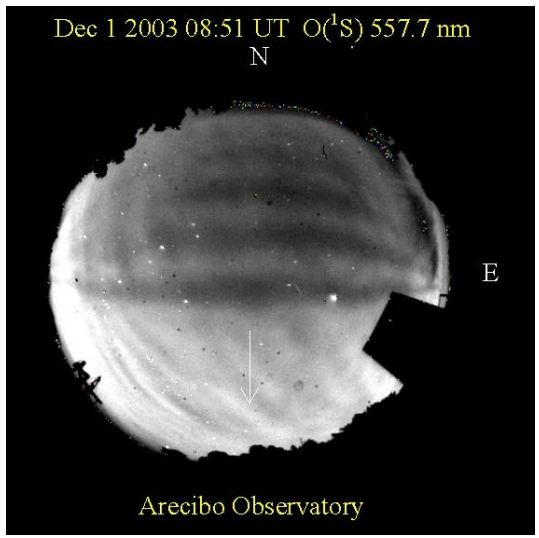

* Extensive band-like patterns that exhibit a sudden or sharp onset. Propagate at 50-70 ms^{-1} and horizontal λ of 25-35 km.

* Bores propagate horizontally inside a ducting region such as a temperature inversion layer or a wind shear.

Courtesy of S. Smith

Equatorial ionospheric irregularities, equatorial spread-F, ESF

* At the magnetic equator gravity and N_e gradients perpendicular to the almost horizontal **B:**

Rayleigh-Taylor instability can develop

$$A(t) = A_o + \delta A e^{\gamma t}$$

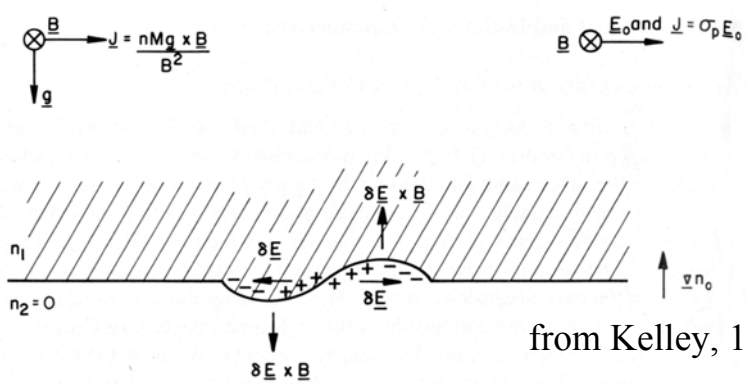

from Kelley, 1989

$$\gamma_{RT} = \frac{\Sigma_P^F}{\Sigma_P^E + \Sigma_P^F} \frac{\vec{\nabla} N}{N} \cdot \left[\frac{\vec{E} \times \vec{B}}{B^2} - \frac{\vec{g}}{\nu_{in}} - \vec{U}_n \right]$$

All the quantities are flux tube integrated

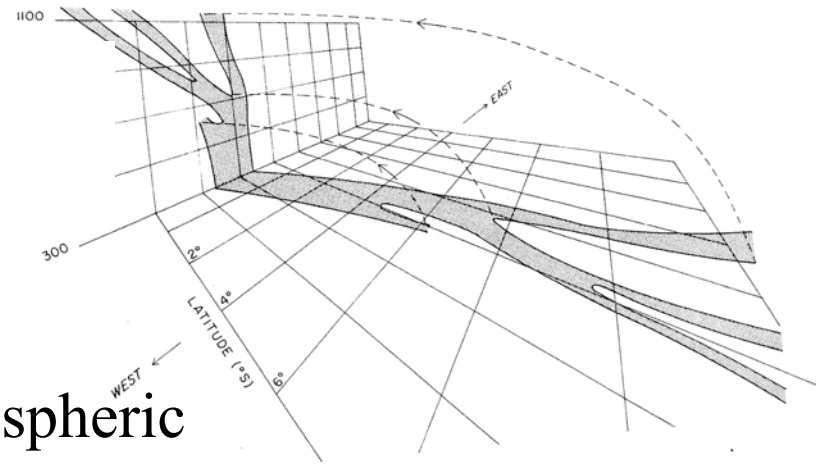

Any Latitude/altitude variations of thermospheric winds, drifts, and conductivities will affect the behavior of the electrodynamics of the system

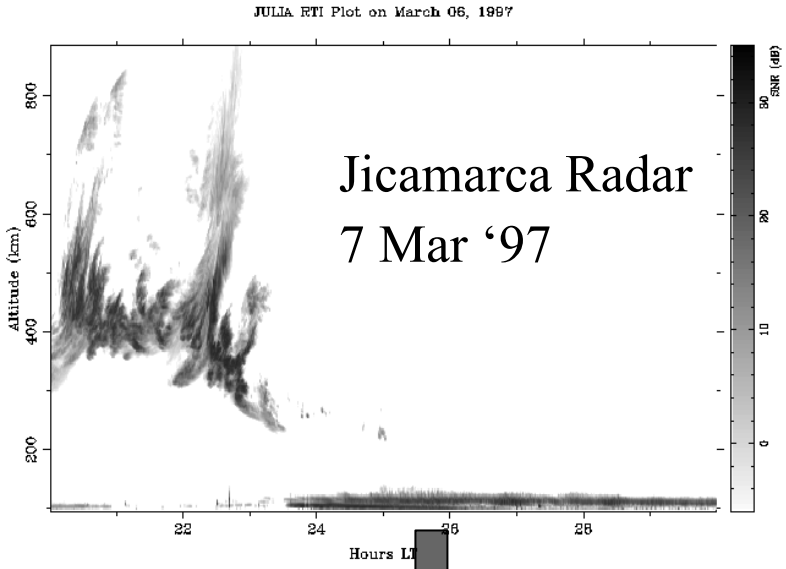

Jicamarca Radar
7 Mar '97

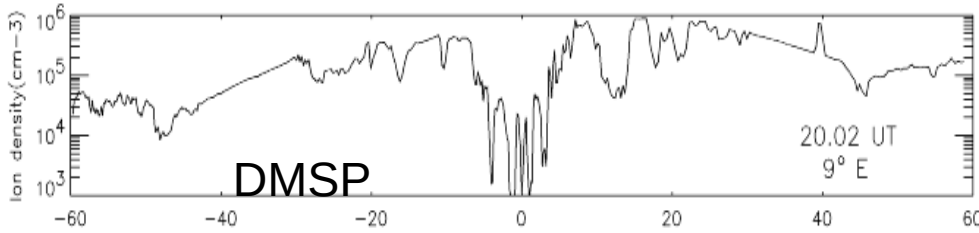

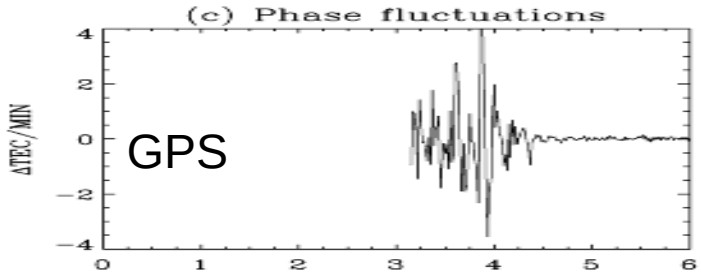

Irregularities are occurring in a scale size spanning at least five order of magnitudes, from 1 m to 10^5 m

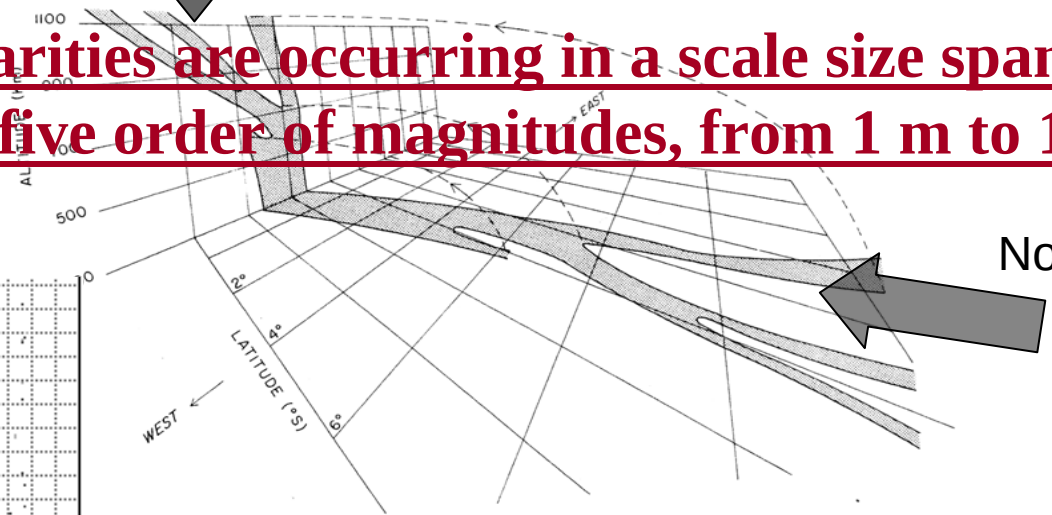

Ionosonde

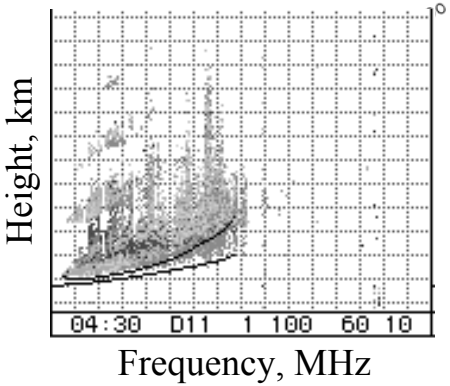

North

East

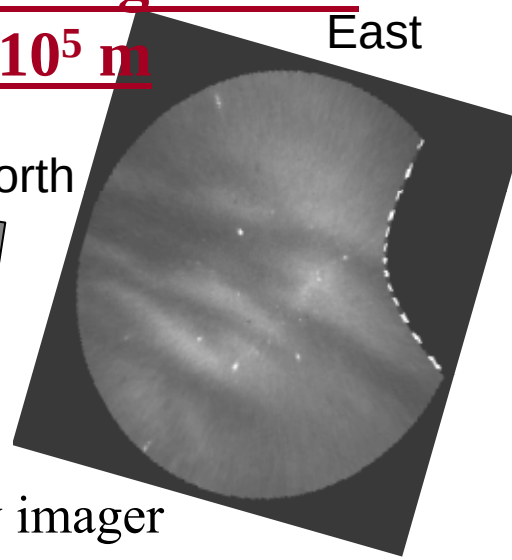

6300 Å all-sky imager
Tucuman 7 Mar '97

ESF structures

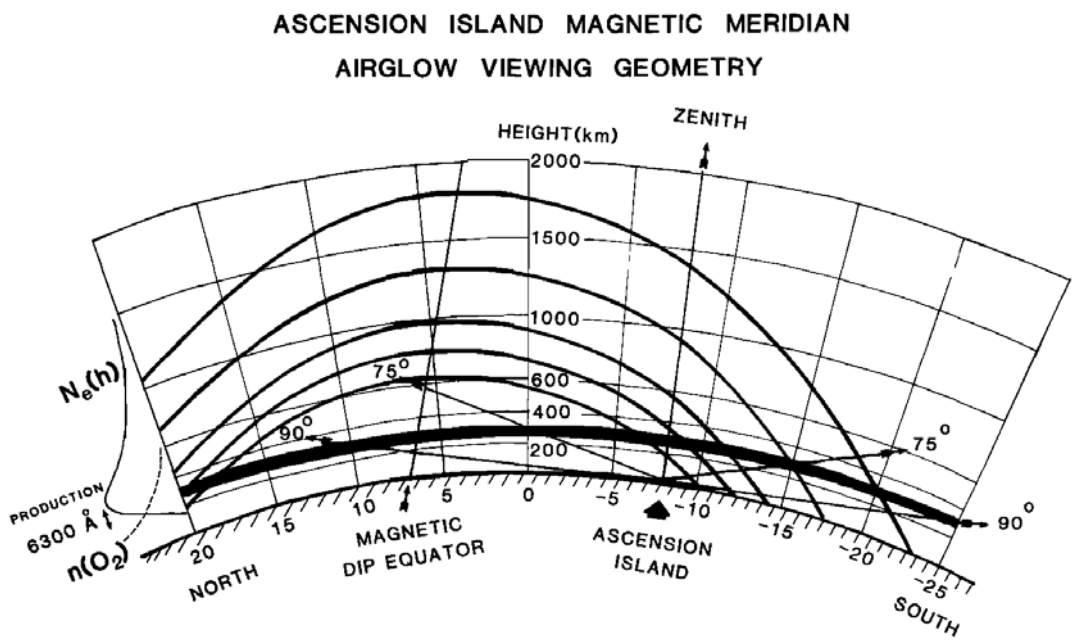

www.buimaging.com

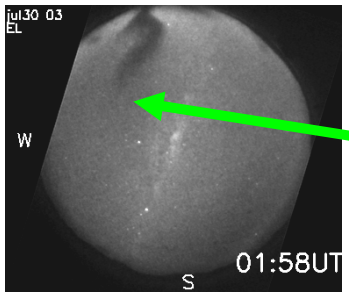

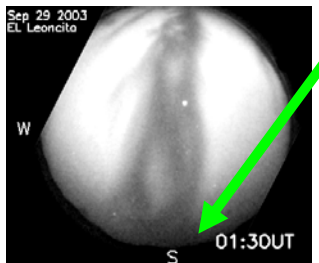

El Leoncito (31º S, -18ºmag)

~900 km Apex height

~1700 km Apex height

Arecibo (16º N, 23º mag)

~1800km Apex height

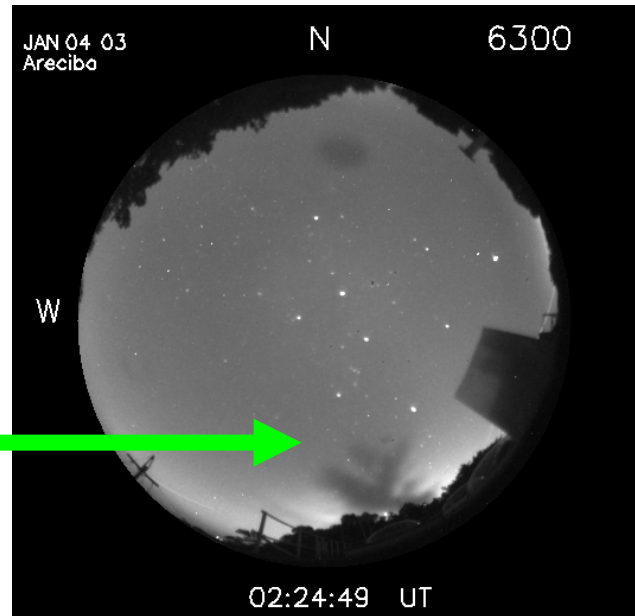

Zonal drift from all-sky images

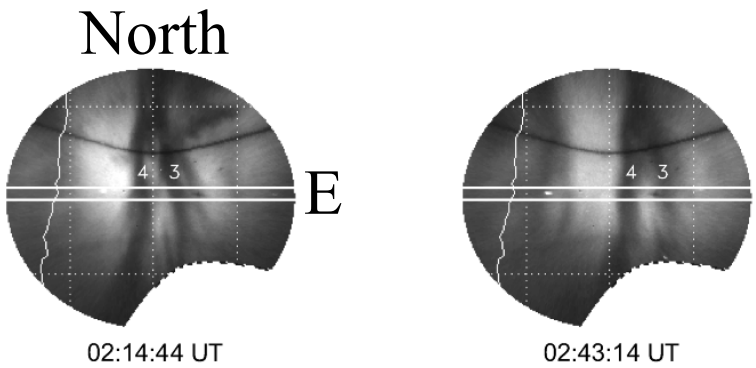

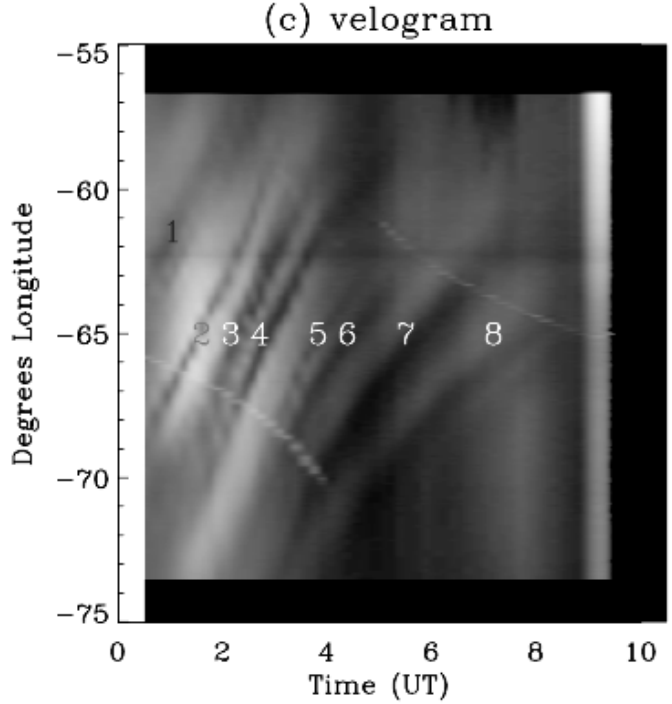

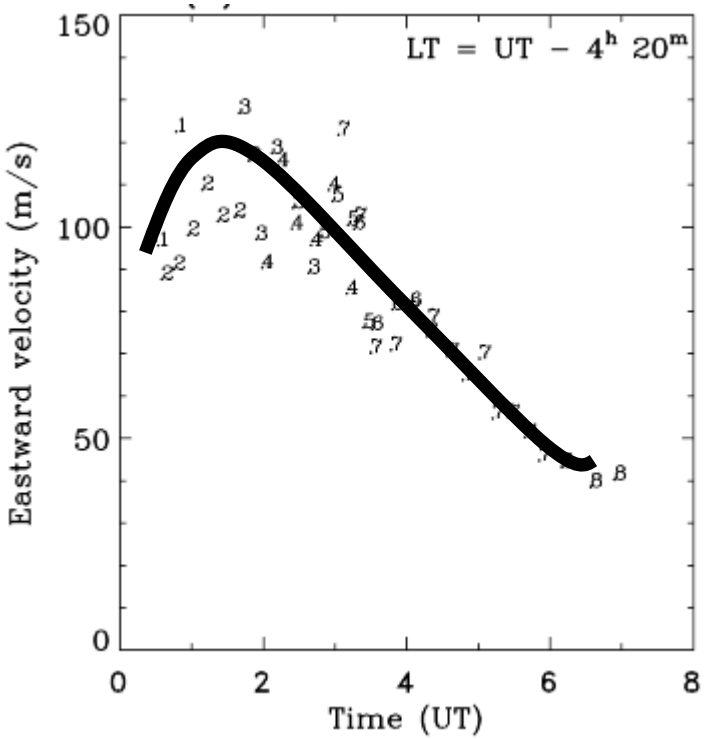

(from Martinis et al., 2003)

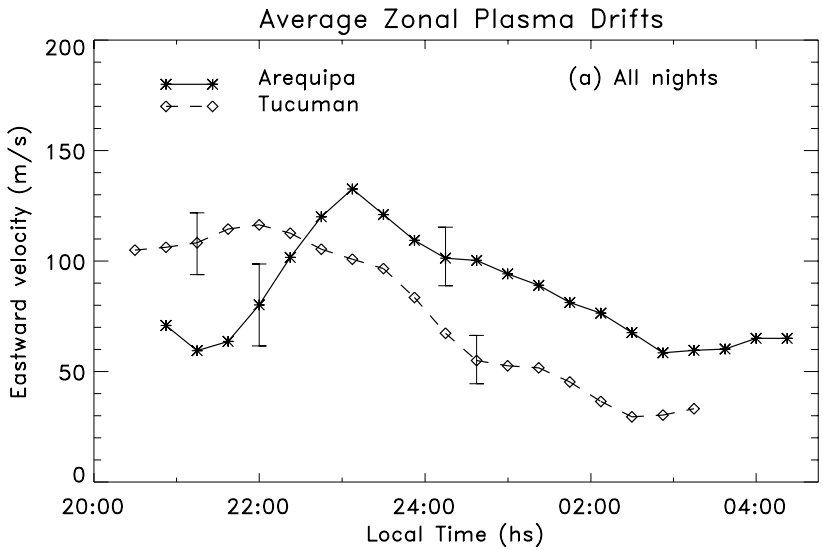

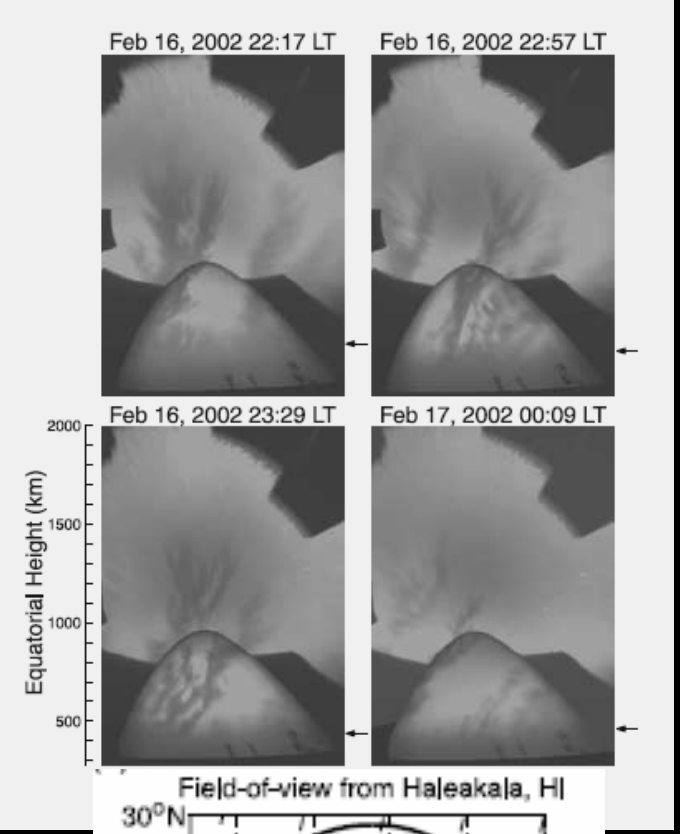

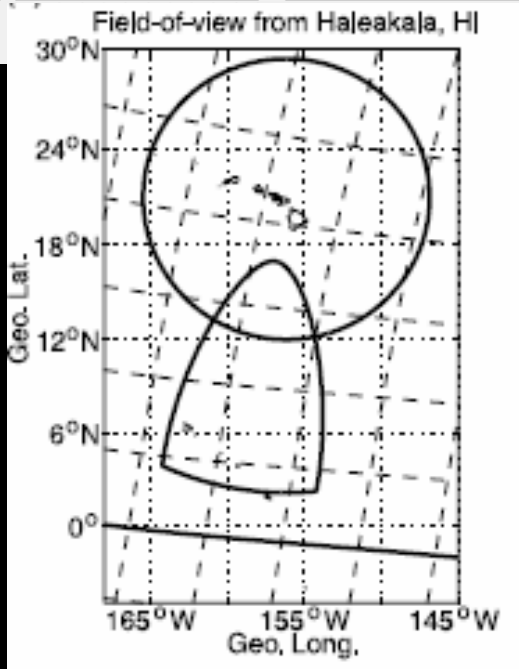

from Kelley et al., ‘02

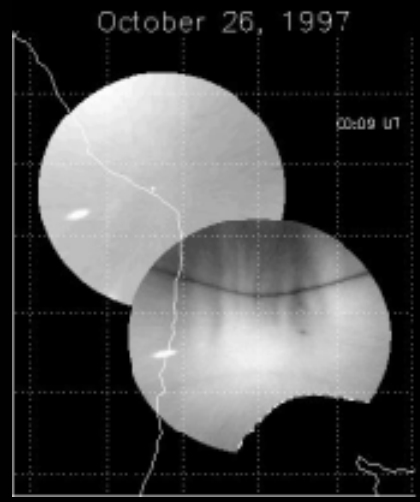

from Martinis, ‘06

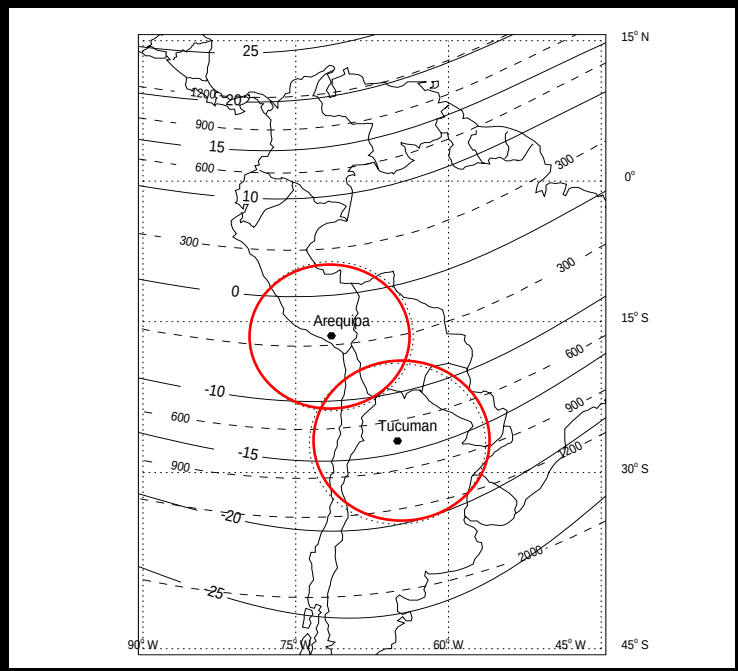

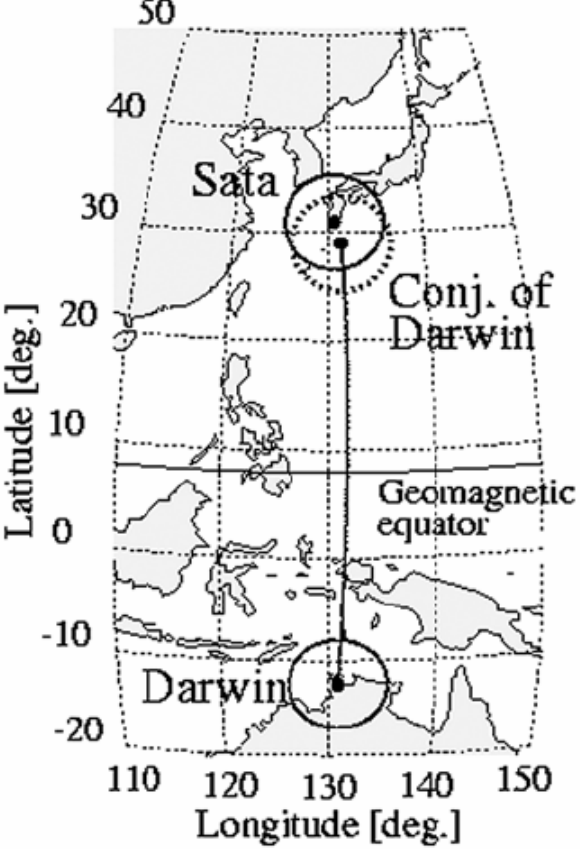

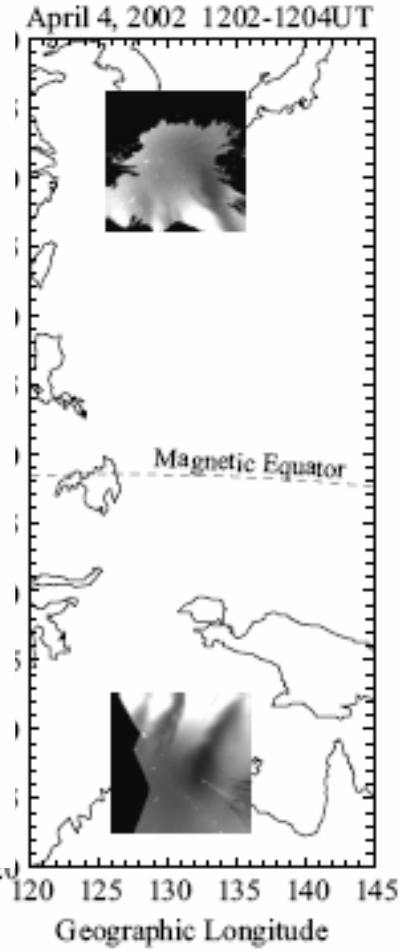

Otsuka et al. (GRL, 2002)

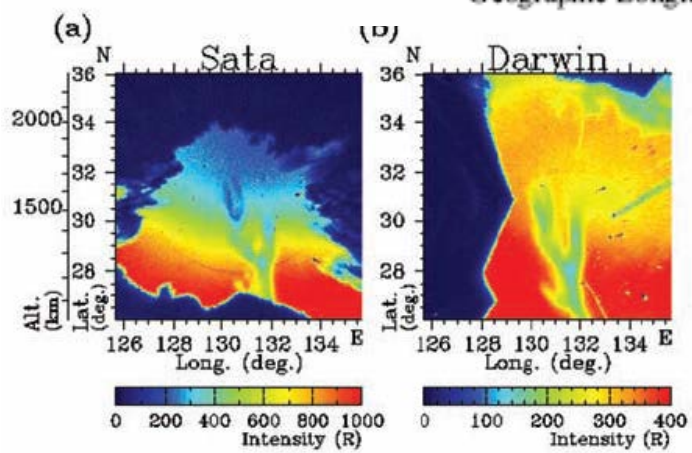

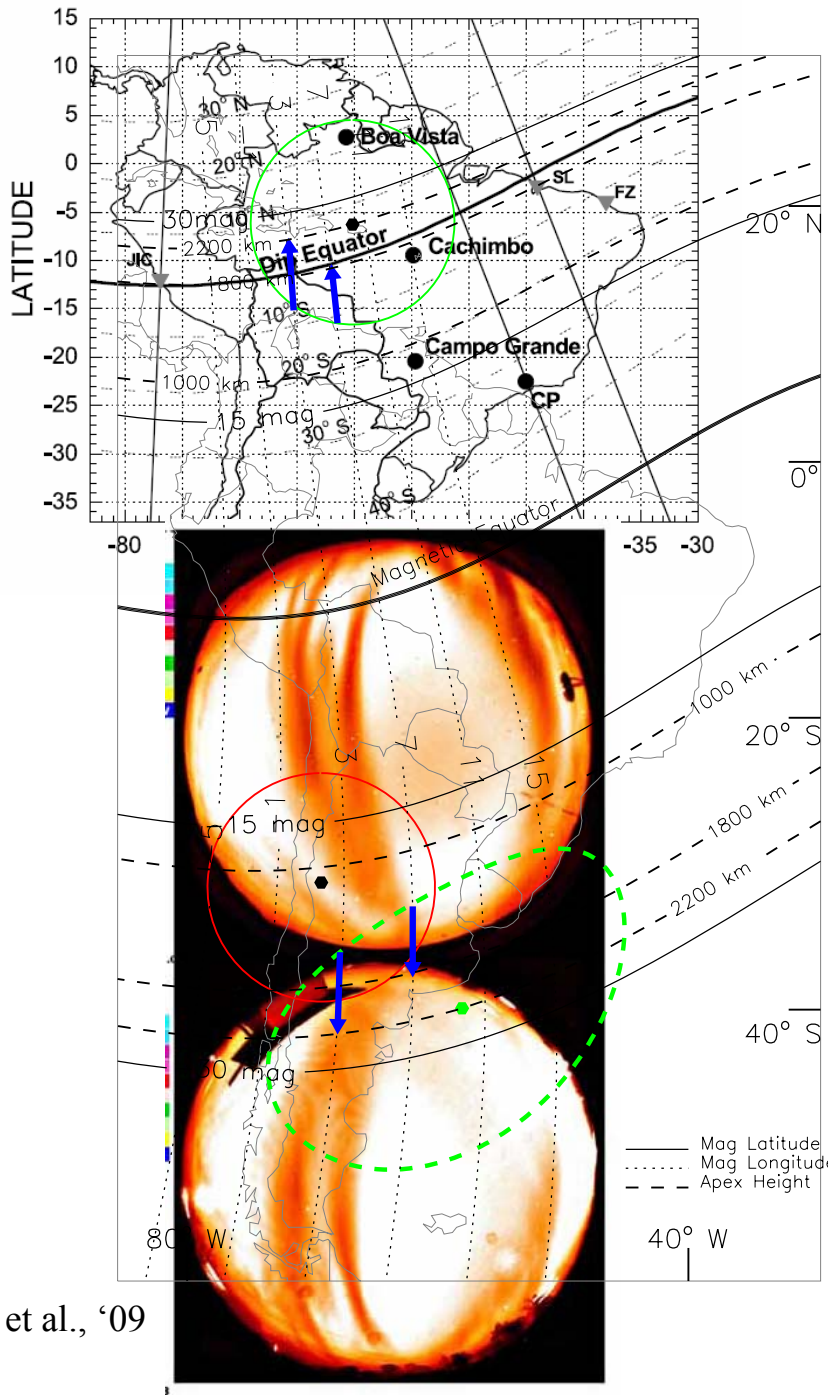

Abdu et al., '09

Conjugate observations (Martinis, JGR'07)

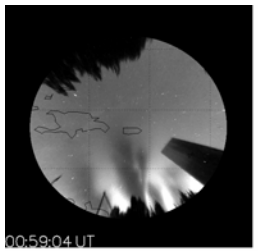

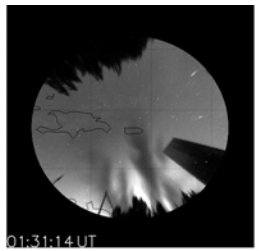

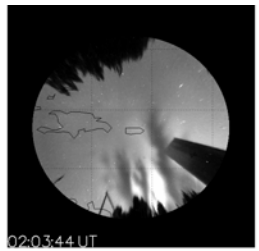

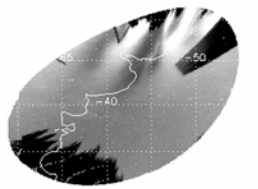

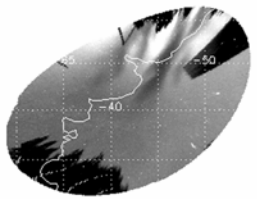

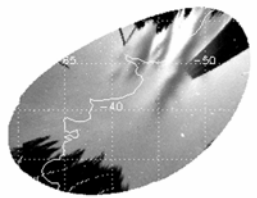

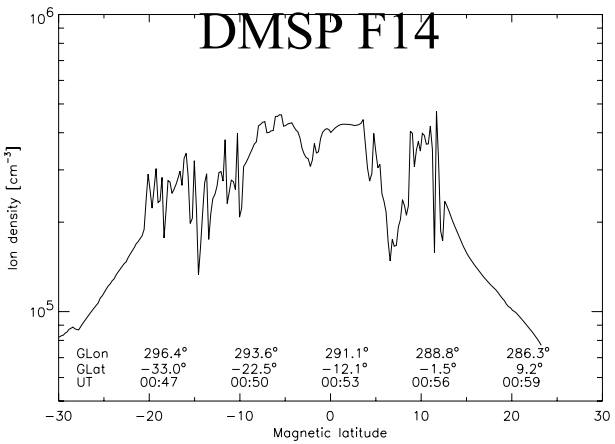

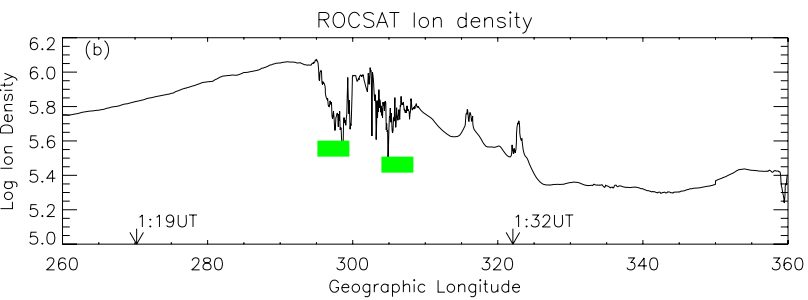

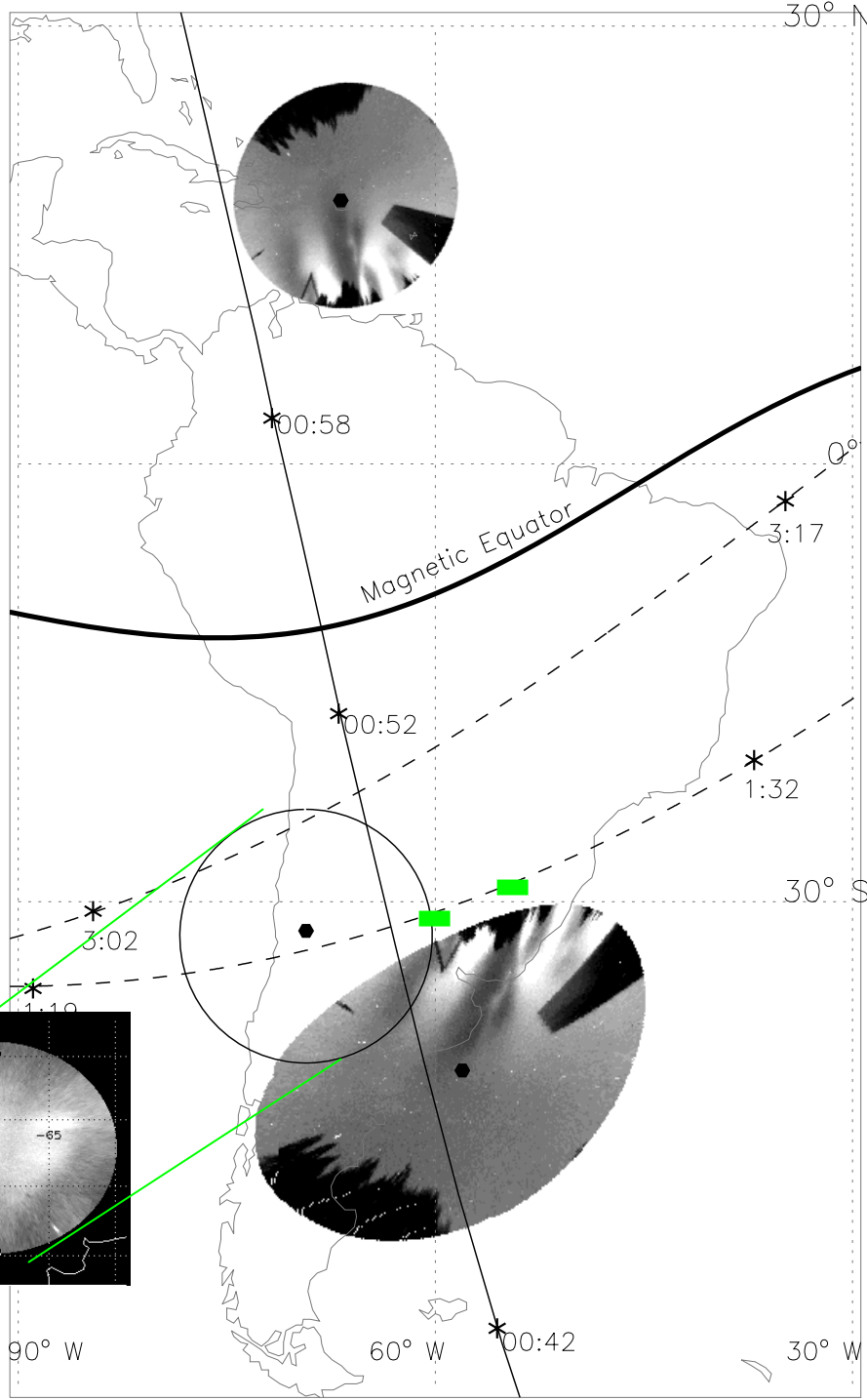

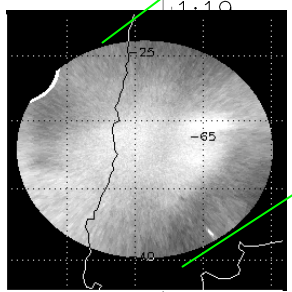

Feb 05 2005

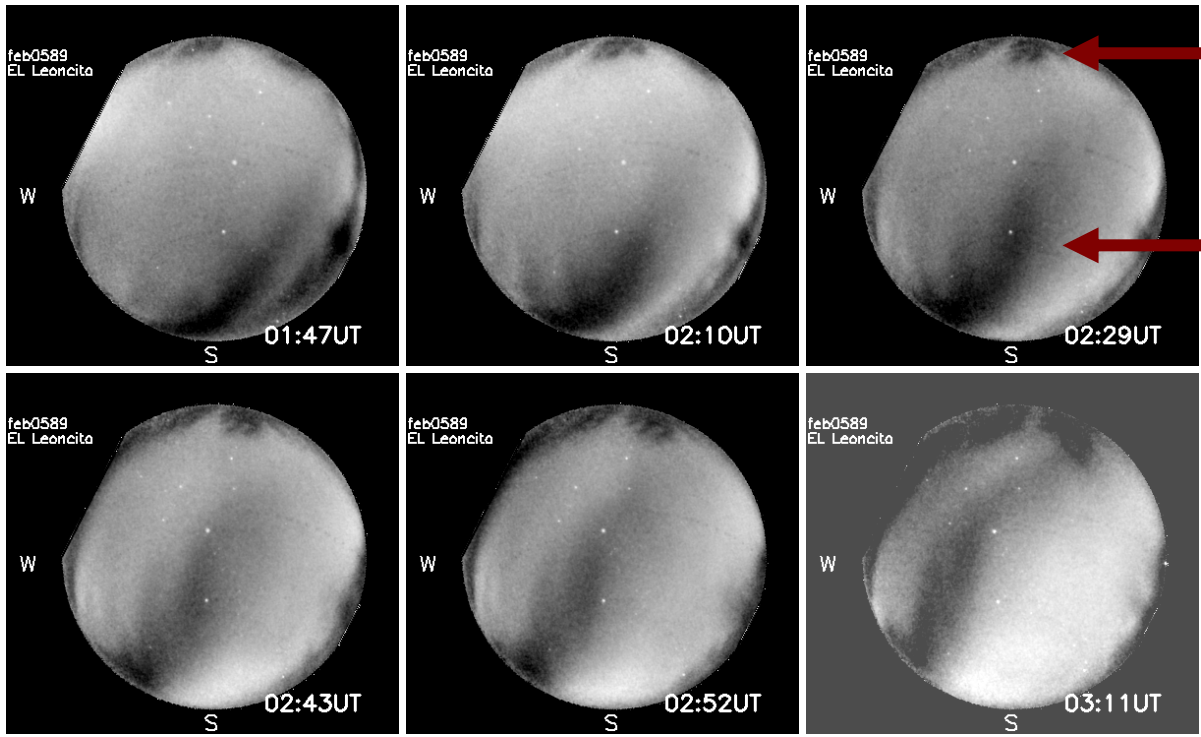

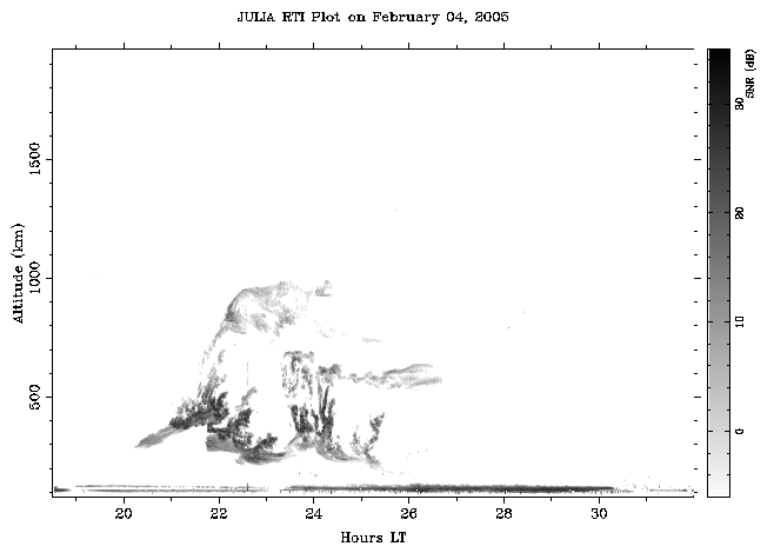

Simultaneous occurrence

ESF to the north moving eastward

Dark band moving northwestward

MSTIDs in airglow images

MSTIDs (medium-scale traveling ionospheric disturbances)
gravity waves; Perkins instability; Es-F region coupled instabilities;

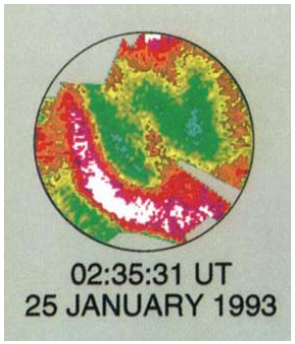

(Mendillo et al., ’97)

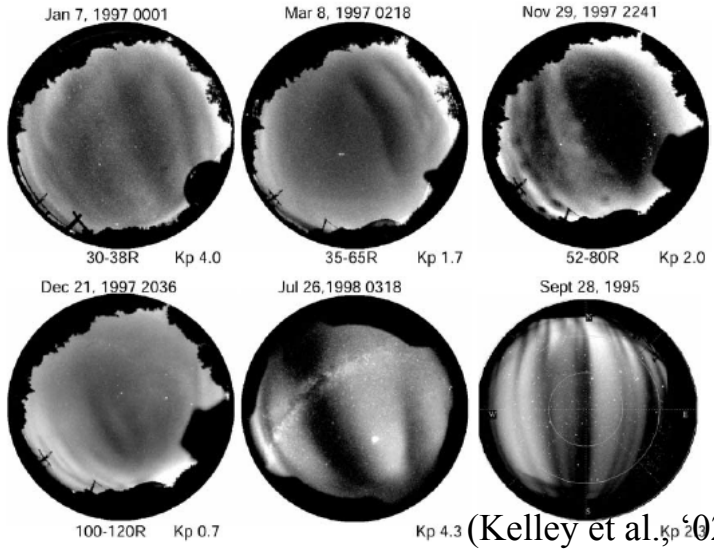

(Kelley et al., ‘02)

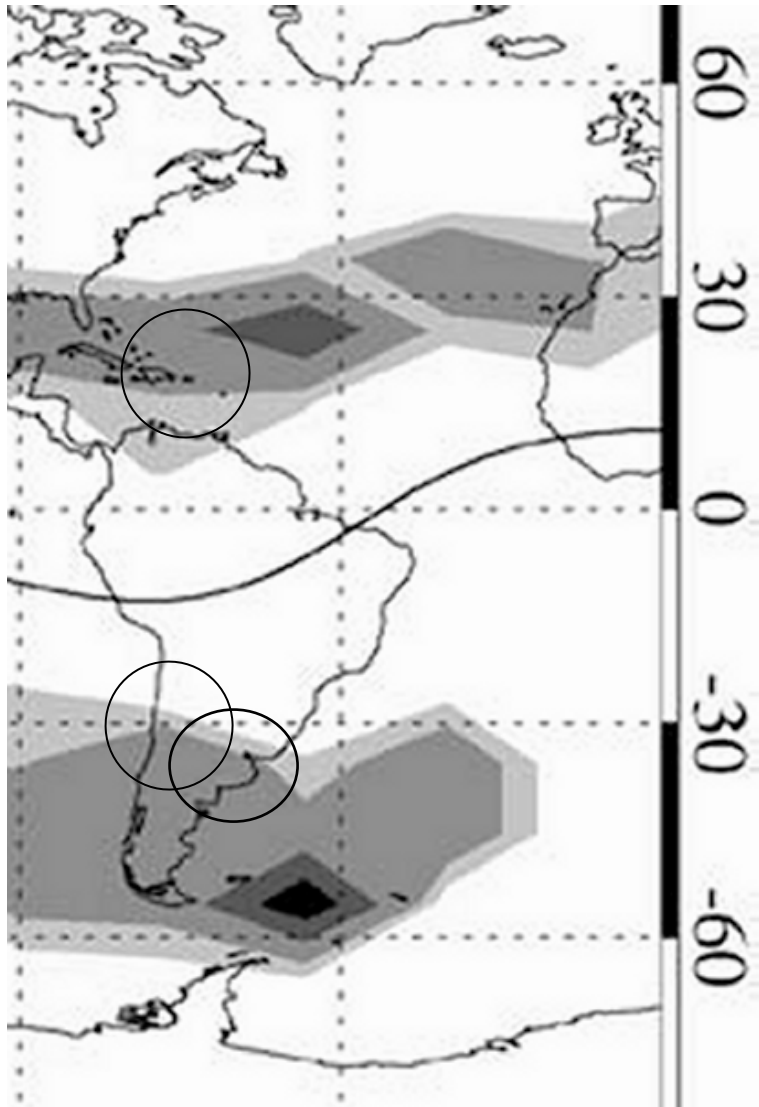

*** Conjugacy of MSTIDs; Propagation limit; associated with electric field fluctuations**

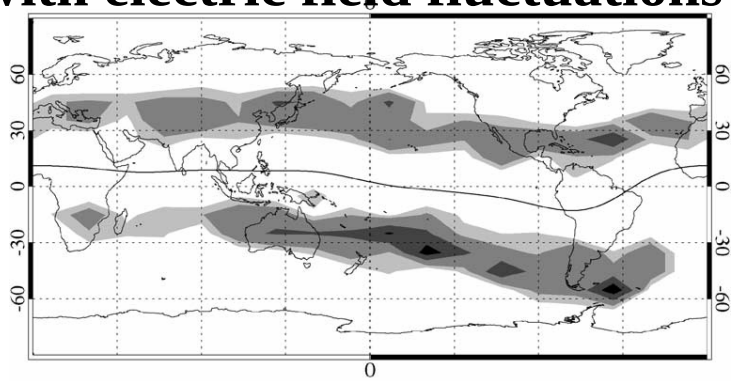

(Saito et al, ‘95).

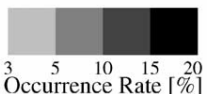

TEC and 6300 waves

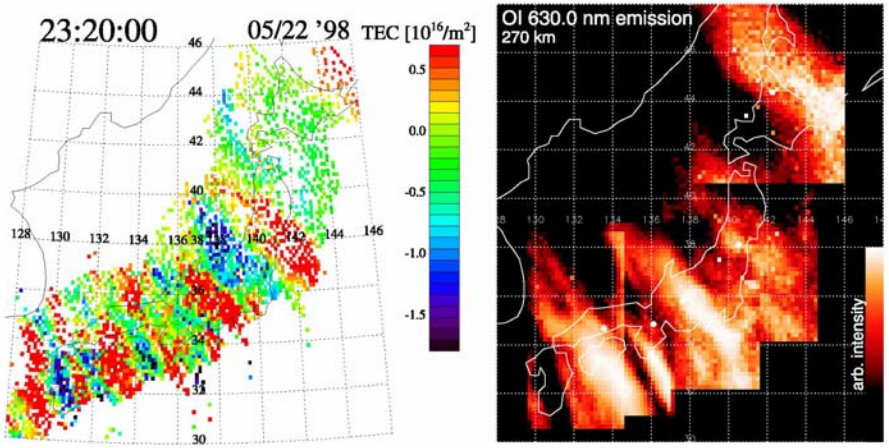

MSTIDs conjugacy

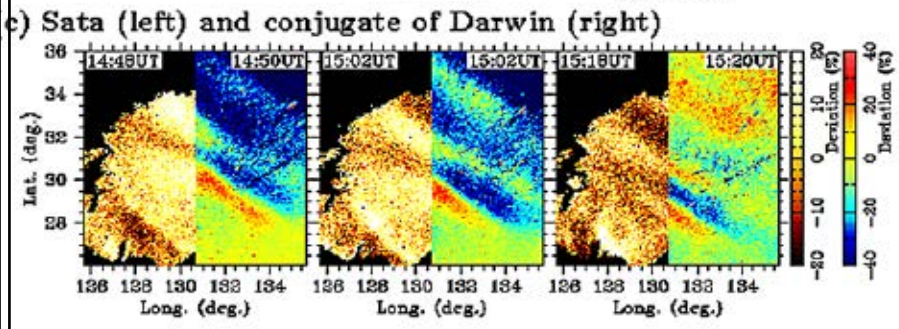

(from Saito et al., 2001)

DMSP electric fields and MSTIDs

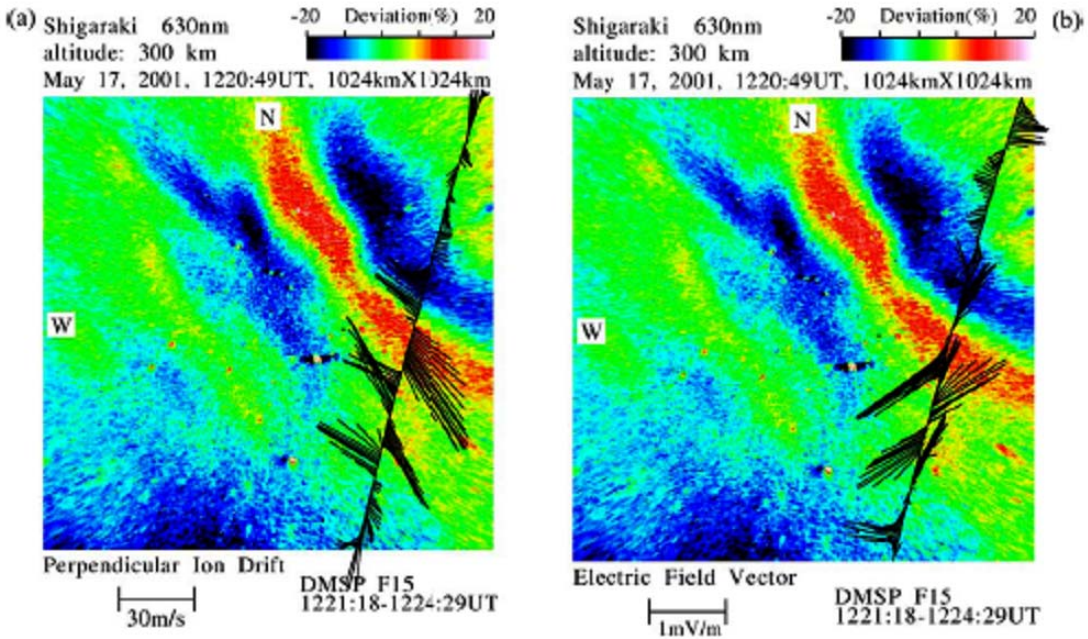

(from Shiokawa et al., 2003)

6 December 2007- El Leoncito **MSTIDs**

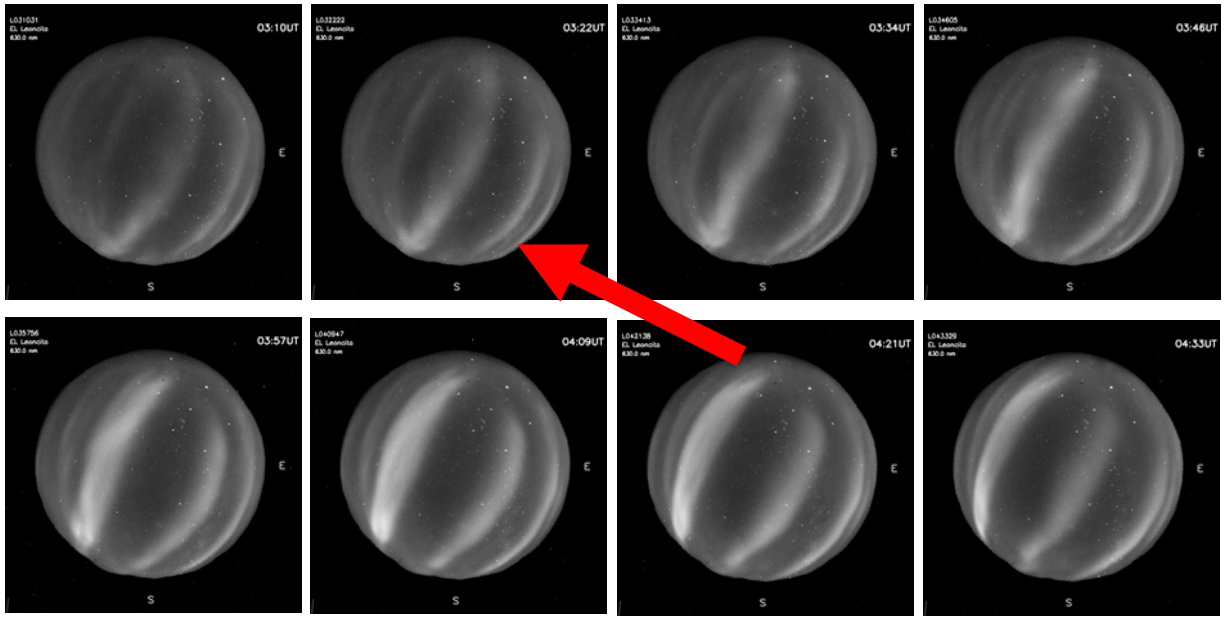

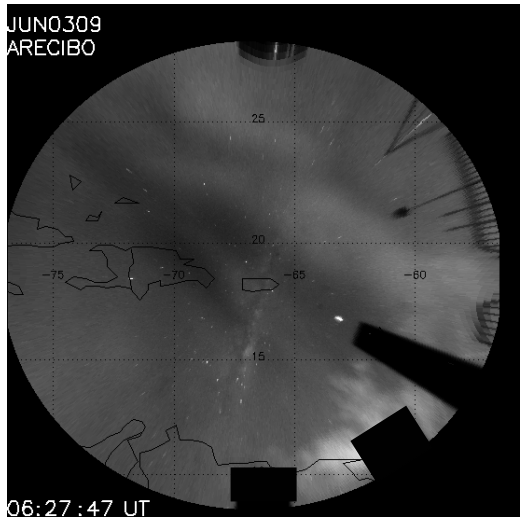

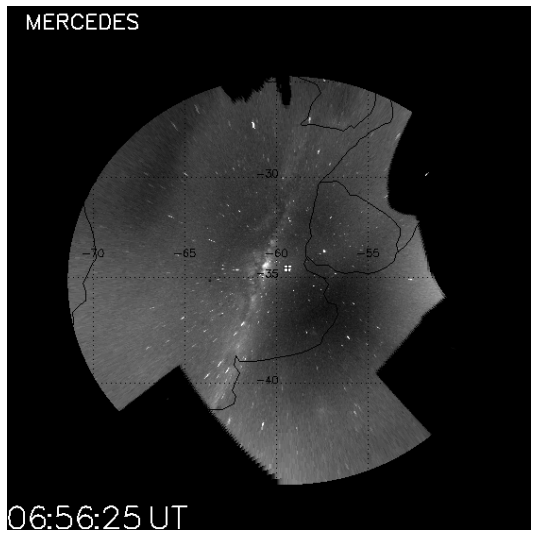

3 June 2009

Arecibo-Mercedes **MSTIDs**

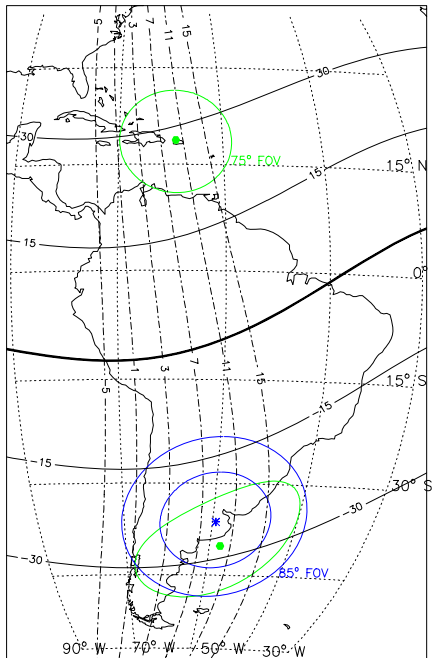

Brightness Wave (optical signature of the MTM)

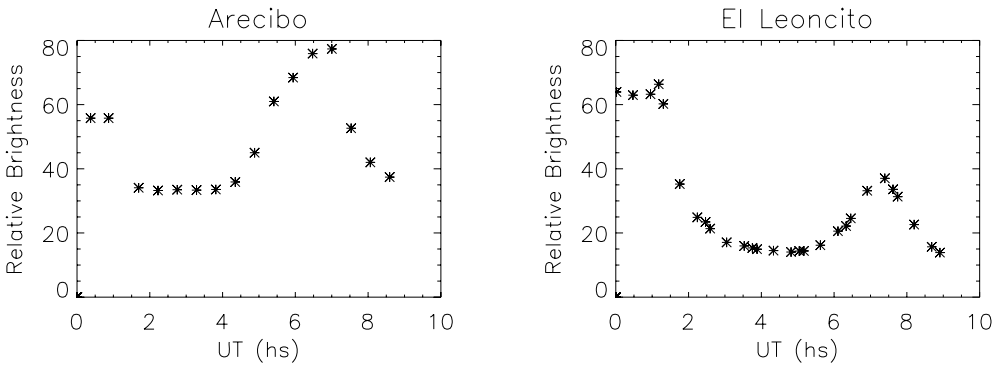

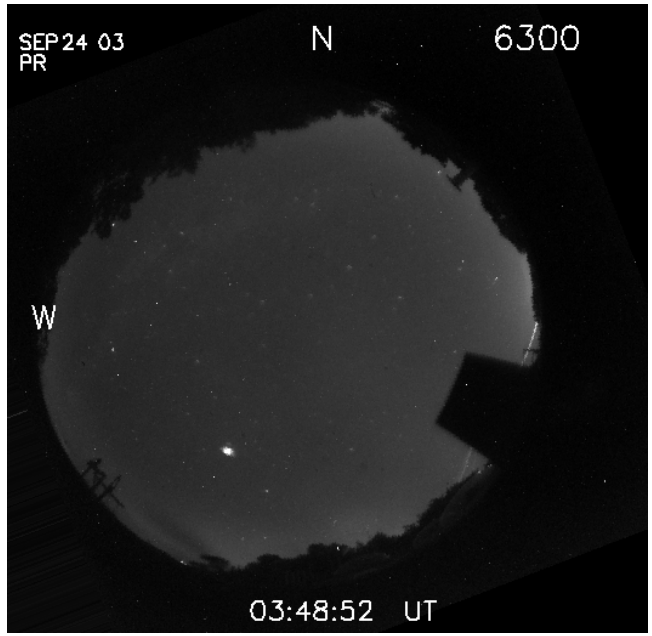

September 24, 2003

* Arecibo: SE to NW

from ~ 4:30 to 7:30 UT

* El Leoncito: NE to SW

from ~ 6:00 to 8:30 UT

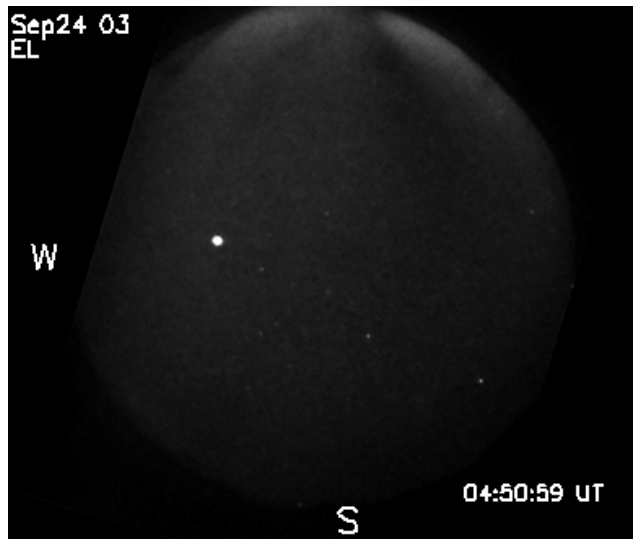

(from Martinis et al., 2006)

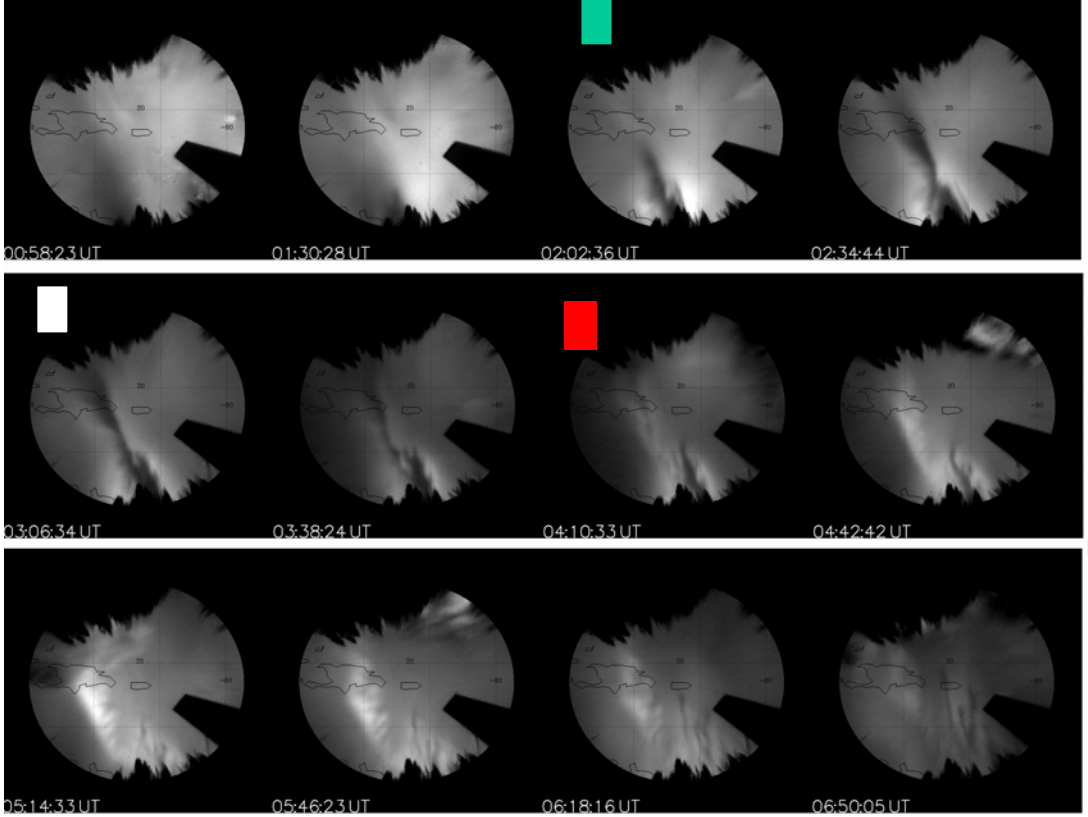

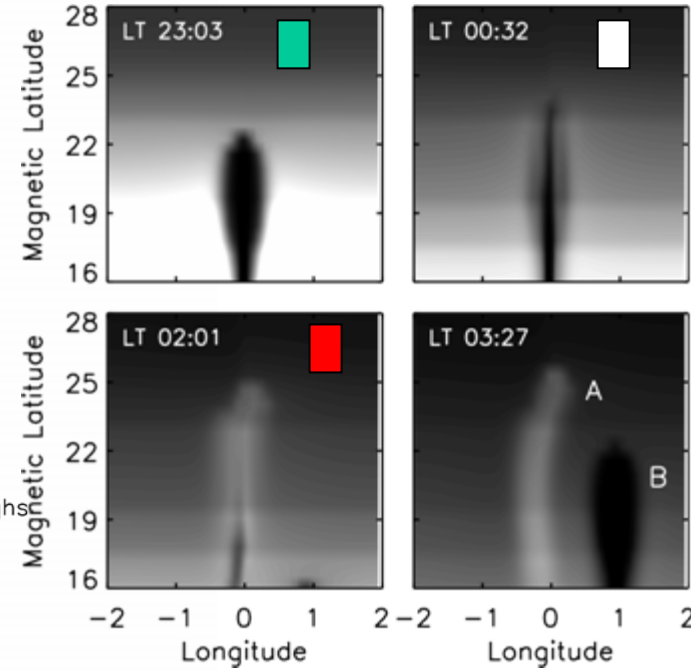

Adapted from Krall et al., 09

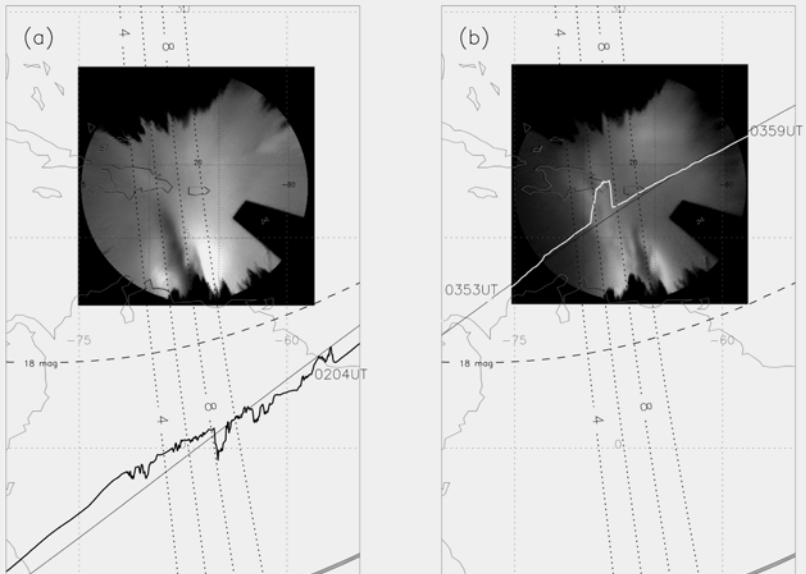

Brightening of a previously dark airglow structure. Comparison with DMSP data and SAMI3/ESF model.

From Martinis et al., ‘09

Using narrow field of view imagers and arrays of imagers

Equatorial studies: CCD cameras looking along B in combination with all-sky imagers; combining all-sky imagers

Auroral studies: ICCDs and EMCCDs

Sprites studies: ICCDs 1000 to 10000 frames per second.

Beyond the Earth's atmosphere: Na spot studies, planetary imaging

Arrays of imagers

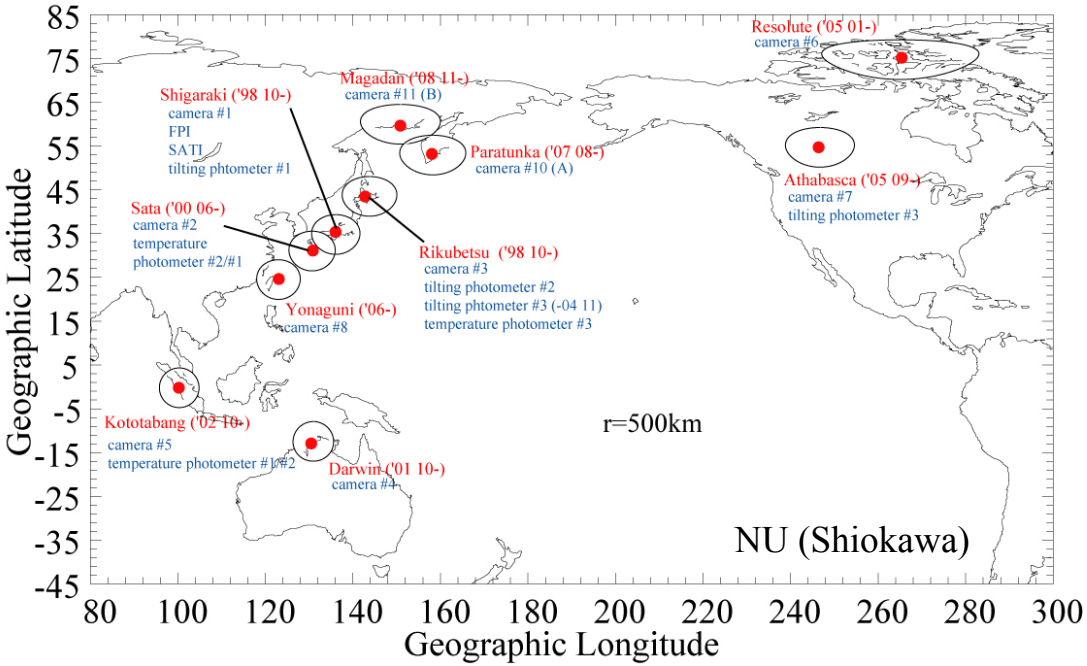

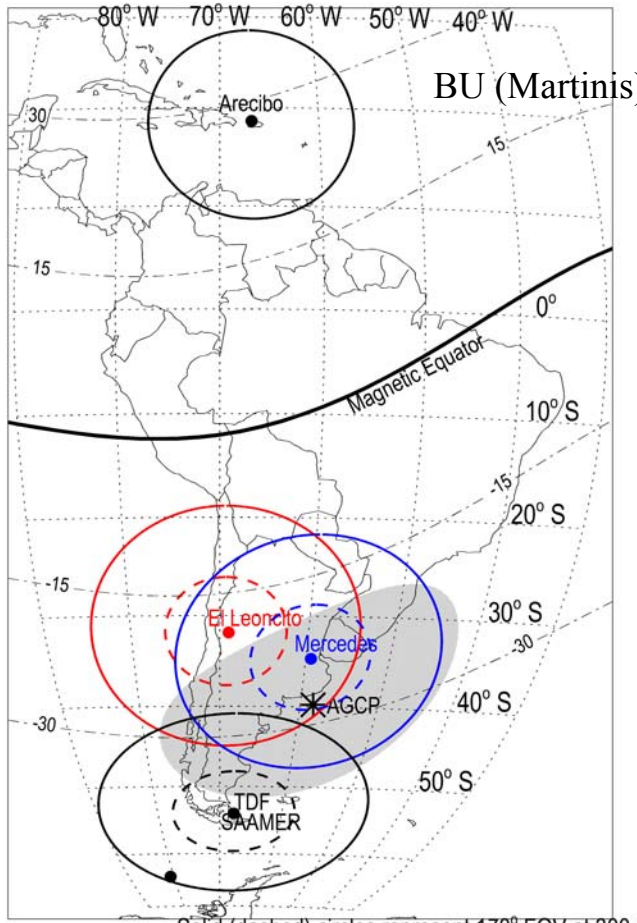

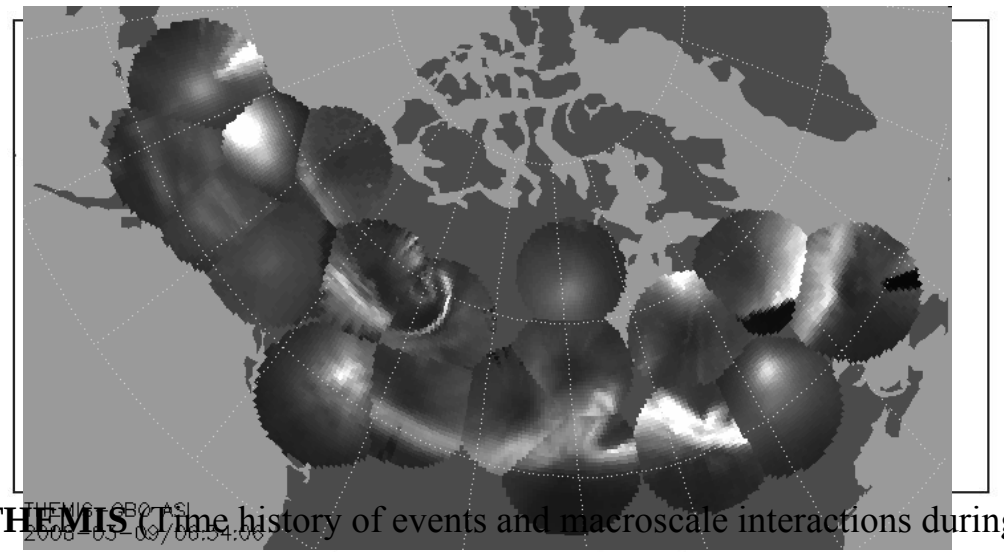

THEMIS (Time history of events and macroscale interactions during substorms)

UC (Donovan)

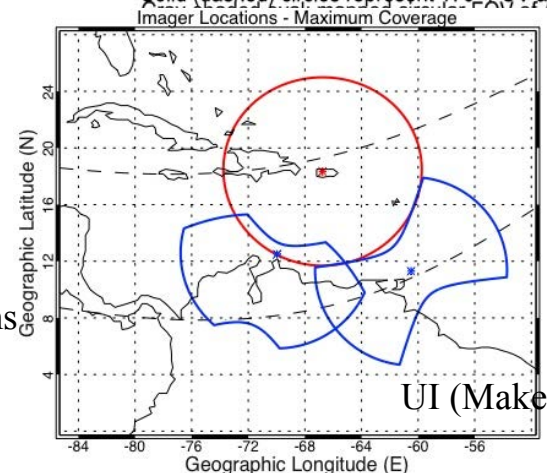

UI (Makela)

Auroral breakup: scale dependence

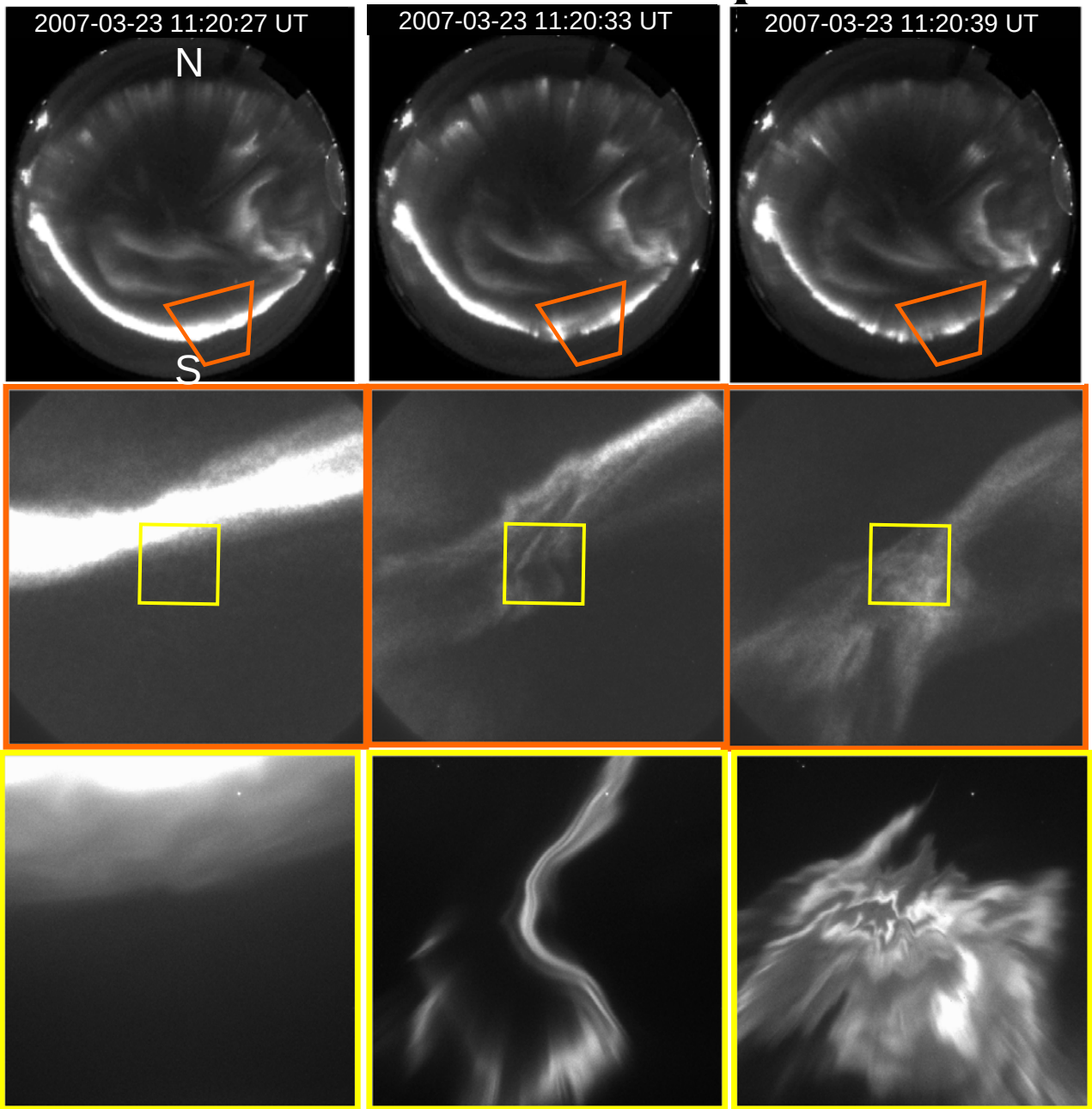

- 180º FOV (~650 km)
- White light
- 1-s exposure

- 30º FOV (65 km)
- N^+_2 427.8nm
- 5-s exposure

- 9º FOV (19 km)
- Prompt emissions
- 33-ms exposure

Semeter et al., 2008

Red Sprites

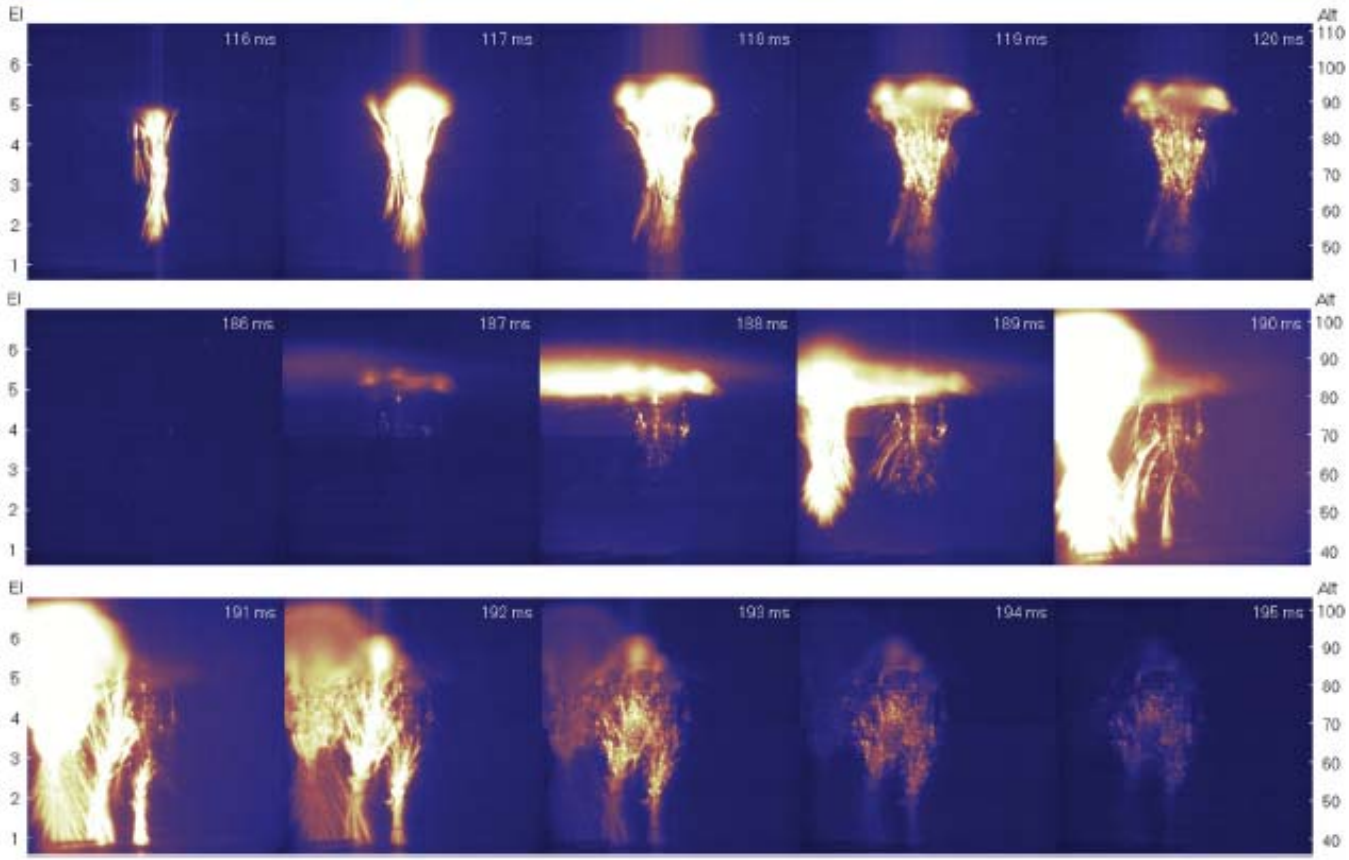

Stenbaek-Nielsen and McHarg, 2008

Phantom-7 high-speed CCD camera with a VideoScope gated intensifier captured these sequence of images in 2005. The intensifier has a P-24 phosphor with a decay time constant of a few ns so there is no persistence between successive images (older model, 0.8 ms decay time constant). FOV each frame is 6^o x 6^o

* During new Moon time, the geometry of the Sun, Moon and Earth is such that the anti-sunward sodium flux is perturbed by the terrestrial gravitational field resulting in its focusing into a dense core

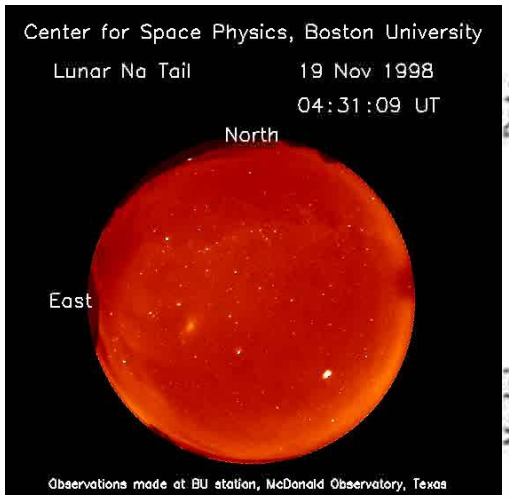

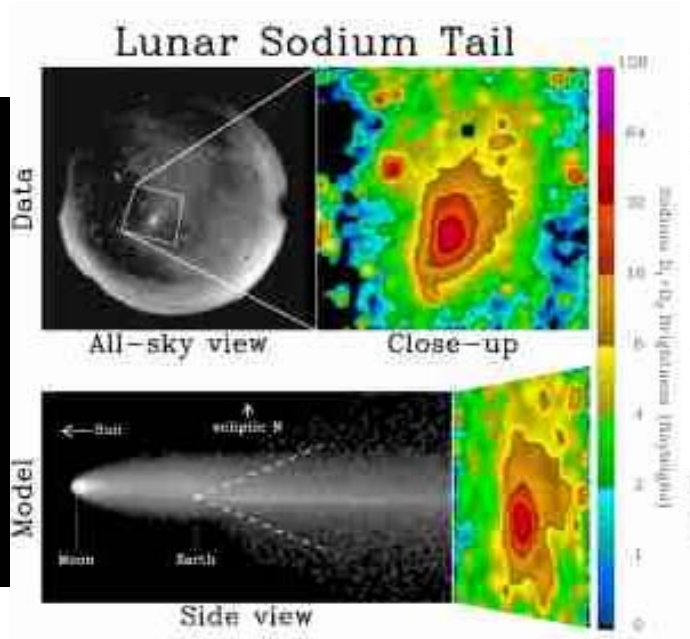

Wilson et al., 1999

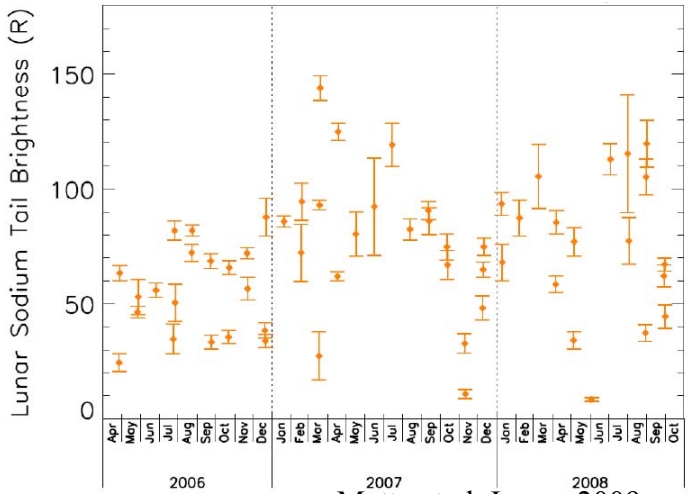

Matta et al.,Icarus 2009

* At the McDonald Observatory, a 10-cm aperture telescope equipped with coronagraphic capabilities has been developed to obtain low-light-level, wide-angle (~7° FOV), narrow-band filtered images of sodium exospheres at Io, the Moon and recently, Mercury.

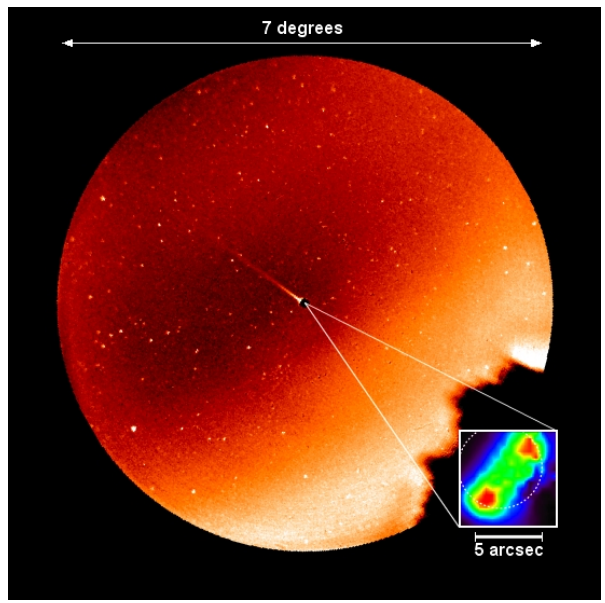

Baumgardner et al., GRL, 2009

Summary

- Since the first observations in the late ’70s optical imaging of atmospheric processes has become a pivotal tool for aeronomy.

- All-sky imagers allow us to study the 2D structure of mesospheric and thermospheric processes, in particular they separate spatial and temporal evolution.

- The optical diagnostics is enhanced when complementary instrumentation is used.

- Narrow field of view imagers can be used to study processes with a better spatial resolution; they can also be applied to investigate processes occurring beyond the Earth’s atmosphere.